
Article:
Wilson, S., Johnson, M.P. and Ruban, A.V. (2021) ΔpH dominates proton motive force in plant photosynthesis in both low and high light. Plant Physiology, 187 (1). pp. 263-275. ISSN 0032-0889

https://doi.org/10.1093/plphys/kiab270

Research Article

Short title

Unravelling the transthylakoid proton motive force

Alexander V. Ruban
School of Biological and Chemical Sciences
Queen Mary University of London
Fogg Building, Mile End Road
LONDON, E1 4NS
United Kingdom
tel.: +44(0)2078826314
a.ruban@qmul.ac.uk

ΔpH dominates proton motive force in plant photosynthesis in both low and high light

Sam Wilson[1], Matthew P. Johnson[2], and Alexander V. Ruban[1*]

[1]School of Biological and Chemical Sciences, Queen Mary University of London, Mile End Road, London, E1 4NS, United Kingdom

[2]Department of Molecular Biology and Biotechnology, University of Sheffield, Sheffield, S10 2TN, United Kingdom

One sentence summary

Electrochromic shift absorption kinetics show the steady-state transthylakoid proton motive force in plants is dominated by the proton concentration gradient under both low and high light conditions.

Author contributions

M.P.J., A.V.R., and S.W. designed the research, S.W. and M.P.J. carried out the experimental work, and all authors analysed and discussed the data and contributed to the writing of the manuscript.

*The author responsible for distribution of materials integral to the findings presented in this article in accordance with the policy described in the Instructions for Authors (www.plantphysiol.org) is: Alexander V. Ruban, a.ruban@qmul.ac.uk

Funding information

This work was supported by Office of The Royal Society Wolfson Research Merit Award (WM140084), a BBSRC grant [BB/L019027/1] to A.V.R. M.P.J. acknowledges funding from the Leverhulme Trust grant RPG-2019-045.

Abstract

The proton motive force (*pmf*) across the thylakoid membrane couples photosynthetic electron transport and ATP synthesis. In recent years, the electrochromic carotenoid and chlorophyll absorption band shift (ECS), peaking ~515 nm, has become a widely used probe to measure *pmf* in leaves. However, the use of this technique to calculate the parsing of the *pmf* between the proton gradient (ΔpH) and electric potential (Δψ) components remains controversial. Interpretation of the ECS signal is complicated by overlapping absorption changes associated with violaxanthin de-epoxidation to zeaxanthin (ΔA505) and energy-dependent non-photochemical quenching (qE) (ΔA535). In this study, we used Arabidopsis (*Arabidopsis thaliana*) plants with altered xanthophyll cycle activity and photosystem II subunit S (PsbS) content to disentangle these overlapping contributions. In plants where overlap between ΔA505, ΔA535 and ECS is diminished, such as *npq4* (lacking ΔA535) and *npq1npq4* (also lacking ΔA505), the parsing method implies the Δψ contribution is virtually absent and *pmf* is solely composed of ΔpH. Conversely, in plants where ΔA535 and ECS overlap is enhanced, such as L17 (a PsbS overexpressor) and *npq1* (where ΔA535 is blue-shifted to 525 nm) the parsing method implies a dominant contribution of Δψ to the total *pmf*. These results demonstrate the vast majority of the *pmf* attributed by the ECS parsing method to Δψ is caused by ΔA505 and ΔA535 overlap, confirming *pmf* is dominated by ΔpH following the first 60 seconds of continuous illumination under both low and high light conditions. Further implications of these findings for the regulation of photosynthesis are discussed.

Introduction

Photosynthesis relies upon many interconnected bioenergetic and biochemical processes. Within the chloroplast thylakoid membrane, light energy is used to drive charge separation in the photosynthetic reaction centres, photosystem I and II (PSI; PSII). These photochemical reactions, and the subsequent operation of the Q-cycle within cytochrome b_6f (cytb_6f), result in the movement of electrons and protons across the span of the thylakoid membrane bilayer, generating an electrical potential ($\Delta\psi$) and a chemical gradient of protons (ΔpH) (Kramer et al., 2003; Malone et al., 2021). This electrochemical gradient is known as the *proton motive force* (*pmf*) and is utilised by the thylakoid ATP synthase to drive the endergonic synthesis of ATP in the chloroplast stroma (Nelson and Junge, 2015). According to Mitchell's chemiosmotic theory, $\Delta\psi$ and ΔpH are thermodynamically and kinetically equivalent components of the *pmf* (Mitchell, 1961; Hangarter and Good, 1982) that can be expressed as follows:

$$pmf = \Delta\psi_{i-o} - \frac{2.3\mathrm{RT}}{\mathrm{F}} \cdot \Delta\mathrm{pH}_{o-i}$$

where $\Delta\psi_{i\text{-}o}$ is the electrical gradient (lumen-*minus*-stroma), R is the ideal gas constant, T is the temperature, F is the Faraday constant, and $\Delta\mathrm{pH}_{o\text{-}i}$ is the proton gradient (stroma-*minus*-lumen).

In addition to its central role in cellular energy conservation, the $\Delta\psi$ and ΔpH components of the *pmf* also play important roles in the regulation of photosynthesis (Armbruster et al., 2017). Increased ΔpH acts as the trigger for the major rapidly-reversible component of nonphotochemical quenching (known as 'qE'), which protects PSII from photooxidative damage (Ruban and Wilson, 2020) and for 'photosynthetic control', which protects PSI from overreduction in excess light by regulating the rate of plastoquinol (PQH_2) oxidation at the cytb_6f complex (Suorsa et al., 2013). Increased $\Delta\psi$, in contrast, has been shown to *cause* photodamage in thylakoids by promoting charge recombination between the primary and secondary radical pairs in the PSII RC, chlorophyll triplet formation, and thus generation of singlet oxygen (Bennoun, 1994; Davis et al., 2016, Davis et al., 2017). Consistent with these contrasting effects, a wide range of experimental approaches, including microelectrodes, pH sensitive dyes, and radiolabelling, concluded that the vast majority of *pmf* in chloroplasts is stored as ΔpH due to rapid compensatory counterion movements that dissipate $\Delta\psi$ (Dilley and Vernon, 1965; Bulychev et al., 1972; Rottenberg et al., 1972; Schuldiner et al., 1972; Barber et al., 1974; Pick et al., 1974; Chow et al., 1976; Vredenberg and Bulychev, 1976; Slovacek and Hind, 1981; Bulychev, 1984; Van Kooten et al., 1986; Remiš et al., 1986; Vredenberg, 1997). The preference of chloroplasts for ΔpH was in contrast to the situation in mitochondria where *pmf* is stored mainly as $\Delta\psi$, due to the low ion permeability of the mitochondrial inner membrane, with a ΔpH contribution of only ~0.5 units, approximately 25% of the total mitochondrial *pmf* (Mitchell,

1961; Lambert and Brand, 2004; Mitchell, 2011; Wolf et al., 2019). These differences were rationalised on the basis that since mitochondria utilise chemical reductants, such as NADH and succinate, and consume oxygen through respiration, avoiding charge recombination is unnecessary.

The consensus view that the steady-state transthylakoid *pmf* consists primarily of ΔpH, built largely on work with isolated chloroplasts, was later challenged by the emergence of the electrochromic shift (ECS) signal as an *in vivo* probe of the *pmf* in intact leaves (Kramer and Sacksteder, 1998; Cruz et al., 2001; Kramer et al., 2003). The Δψ component induces an electrochromic band shift (ECS) in the Soret peak absorption of chlorophylls and carotenoids in the thylakoid membrane (Witt, 1971; Witt, 1979; Vredenberg, 1997; Bailleul et al., 2010). This results in the formation of a transient absorption peak ~515 nm upon illumination of leaves (Witt, 1971). Since a significant proportion of the ECS signal persisted during continuous illumination, Kramer and co-workers suggested that *in vivo*, a larger fraction of *pmf* is stored as Δψ than was suggested by the earlier *in vitro* work (Kramer and Sacksteder, 1998; Cruz et al., 2001; Kramer et al., 2003). Interestingly, they found that the parsing of the *pmf* between the Δψ and ΔpH, implied by the ECS measurements, was affected by light intensity and CO_2 availability (Kanazawa and Kramer, 2002; Takizawa et al., 2007). More recently, the generation of mutants deficient in thylakoid-associated ion channels involved in counterion movements, such as the Cl^- channel VCCN1 and the H^+/K^+ antiporter KEA3, have highlighted the crucial importance of *pmf* composition to plant fitness (Carraretto et al., 2013; Armbruster et al., 2014; Duan et al., 2016; Herdean et al., 2016a; Herdean et al., 2016b).

However, while the ECS signal has proven itself a useful probe of the *pmf* amplitude, proton flux and conductivity in leaves, its suitability for probing *pmf* parsing has been questioned (Johnson and Ruban, 2014). The complicating issue is the congested nature of the spectral region where the ECS absorption changes are observed. Overlapping light-driven absorption changes include those due to the de-epoxidation of violaxanthin to zeaxanthin, which produces a large positive band at ~505 nm, hereafter ΔA505 (Yamamoto et al., 1971; Bilger et al., 1989: Ruban et al, 1993) and the qE-related absorption changes ~525 – 540 nm, often called ΔA535 (Bilger and Björkman, 1990). Of these, the qE-related absorption changes are the most problematic since they form and relax relatively rapidly and are thus more difficult to distinguish from the ECS signal. Whilst the cyt *f* redox changes occur on similarly rapid timescales, the related absorption peak is narrow and centred at ~554 nm, with little-to-no overlap with the ECS, Δ505, or Δ535 (Nishio and Whitmarsh, 1993; Metzger et al., 1997). Initially attributed to light scattering changes caused by altered thylakoid structure provoked by ΔpH formation (Murakami and Packer, 1970b; Murakami and Packer, 1970a; Duniec and Thorne, 1977), they were later shown by Resonance Raman spectroscopy to reflect an

absorption change in a sub-population of zeaxanthin, which required the presence of photosystem II subunit S (PsbS) (Ruban et al., 2002). Theoretical work later showed that ΔA535 may arise from zeaxanthin J-dimers formed at the interface of aggregated LHCII proteins in the qE state (Duffy et al., 2010). Interestingly, when zeaxanthin formation is blocked by inhibitors or through the absence of violaxanthin de-epoxidase (VDE), the qE-related absorption peak shifts from 535 nm to 520 - 525 nm, increasing its overlap with the ECS signal (Crouchman et al., 2006; Johnson et al., 2009). These observations led Johnson and Ruban (2014) to use the ECS method to assess the parsing of *pmf* in the *lut2npq1* mutant of Arabidopsis (*Arabidopsis thaliana*), which fails to synthesise zeaxanthin and is deficient in qE, removing much of the signal contamination from the ECS absorbance window. The data demonstrated that components of the ECS signal could be separated by their differing temporal, Δψ, and ΔpH dependence. In wild-type (WT) leaves, the 515 nm signal shows a sharp rise as illumination commences before decaying to less than 50% of its initial amplitude over the next 30 s, this was then followed by a slower secondary rise which stabilised at ~60 - 70% of the initial amplitude, and according to the ECS parsing method, is attributed to steady-state Δψ. The secondary rise of the ECS signal was completely absent in *lut2npq1* and could be eliminated using the H^+/K^+ antiporter nigericin, which collapses ΔpH. These observations led Johnson and Ruban (2014) to propose that the steady-state Δψ in the WT was caused by the overlapping qE-related absorption change.

In the following study, we widened our investigation into the origin of the steady-state ECS signal to include a range of Arabidopsis plants with altered xanthophyll cycle and PsbS content. Unlike our previous measurements, these data were obtained on the widely used Walz Dual-PAM device with the P515 emitter/detector modules (Klughammer et al., 2013). The results support the original view in the literature that the steady-state Δψ contribution to the *pmf in vivo* is negligible (< 10%), and that the secondary rise in the ECS signal reflects the contribution of the overlapping qE-related absorption changes.

Results

Characterisation of the electrochromic shift, xanthophyll cycle, and qE-related signals in wild-type Arabidopsis leaves

According to the ECS parsing method (Kramer et al., 2003) the light-to-dark transients of the 550 – 515 nm absorption difference signal provide information on the relative contributions of the $\Delta\psi$ and ΔpH to the *pmf*. However, this section of the absorption spectrum is heavily congested with light-induced absorption changes. Fig. 1A shows a selection of such changes. De-epoxidation of violaxanthin to zeaxanthin causes the appearance of a large positive band at ~505 nm, whilst the PsbS-dependent red-shift of a sub-population of zeaxanthin during qE causes an absorption peak at ~535 nm (Ruban et al., 2002; Johnson et al., 2009; Johnson and Ruban, 2009). The ECS-related peak is formed within microseconds of illumination and has its peak at ~515 nm. The qE-related peak forms in seconds to minutes depending on the pre-illumination history of the leaf and can vary in magnitude and position, according to the xanthophyll content of the leaf, as shown in Fig. 1B (Johnson et al., 2009). Whilst the WT peak appears at 534 nm, in the absence of zeaxanthin in the *npq1* mutant, this peak becomes blue-shifted, here shown to be at 523 nm. In the *npq2* mutant, where zeaxanthin is constitutively present, the qE peak becomes red-shifted relative to WT, with its peak appearing at 538 nm. The PsbS-overexpressor, *L17*, possesses a much greater qE response, and this is reflected in the larger magnitude of its qE-related peak at 532 nm.

Fig. 1C shows an expanded and annotated view of a light-to-dark transition in the ECS signal. After the cessation of illumination, an initial sharp trough forms, which slowly relaxes (~30 s) to a pseudo-baseline in the dark. The total amplitude of the initial trough has been assumed to be proportional to the total *pmf*, as here is termed ECS_t (Klughammer et al., 2013). In WT leaves, the post relaxation pseudo-baseline is at a level between the maximal light signal and the minima of the ECS_t. According to the ECS parsing method, the difference between the pseudo-baseline and the ECS_t will be representative of the total ΔpH and is hereafter termed ECS_{inv}, where the subscript denotes a transient inverse $\Delta\psi$ generated when the continuing efflux of protons through the ATP is not rapidly matched by the movement of other ions upon cessation of illumination (Cruz et al., 2001; Kramer et al., 2003). Finally, the difference between the pseudo dark baseline and the steady state level of the ECS signal just prior to the cessation of illumination is attributed to the $\Delta\psi$ and is termed $ECS_{t\text{-}inv.}$

To investigate this further, WT Arabidopsis leaves were exposed to 8 steps of 3 min illumination followed by 3 min of darkness at intensities of 71, 151, 308, 417, 548, 708, 1128, 1396 µmol photons m^{-2} s^{-1}. Here, the ECS (ΔA 550 – 515 nm) and ΔA535 signals can be measured in parallel, as previously described (Klughammer et al., 2013). Fig. 2A shows a representative ECS kinetic trace of the light titration. Under continuous light flux below the growth light intensity (i.e.

< 190 µmol photons m^{-2} s^{-1}; the first two steps), the steady-state ECS signal rises to a maximum level after ~60 s, before relaxing to a level above the subsequent pseudo-dark baseline (Fig. 2A; Fig. S1). This kinetic behaviour is also observed in the ΔA535 signal, shown in Fig. 2B. During these initial two light stages, the ECS_t reaches a level up to ~50% of its maxima, whilst the ECS_{inv} and $ECS_{t\text{-}inv}$ remain in approximately a 1:1 stoichiometry. At 71 µmol photons m^{-2} s^{-1}, the ECS_{inv} accounts for 67 ± 13% of the total ECS_t, whilst the $ECS_{t\text{-}inv}$ accounts for 33 ± 31% ($P > 0.05$, Student's *t*-test). At 158 µmol photons m^{-2} s^{-1}, the ECS_{inv} accounts for 61 ± 7% of the total ECS_t, whilst the $ECS_{t\text{-}inv}$ accounts for 39 ± 8% ($P > 0.05$, Student's *t*-test). According to the ECS parsing method, this would imply an approximately equal partitioning of the *pmf* between ΔpH and Δψ. At 308 µmol photons m^{-2} s^{-1} and above, the ΔA535 signal ceases to relax in the light phase, as does the steady-state ECS in the light, which shows a stark upward rise in the light. Between 308 and 548 µmol photons m^{-2} s^{-1}, the ECS_t also reaches its maxima. Again, here the ECS_{inv} and $ECS_{t\text{-}inv}$ components remain at similar levels (each ~50% of the maximum ECS_t) with no significant differences between the two ($P > 0.05$; Student's *t*-test). At light intensities of 708 µmol photons m^{-2} s^{-1} and higher, the ECS_t starts to decrease, with the minimum under high light being achieved at 1396 µmol photons m^{-2} s^{-1}, with an ECS_t 84.9 ± 1.7% of the maximum. Furthermore, as the light intensity increases, the ΔA535 signal continues to rise to a maximum level, 42.9% higher at 1396 µmol photons m^{-2} s^{-1} than at 308 µmol photons m^{-2} s^{-1}. Under high light, the ECS_{inv} proportion continues to rise with respect to the $ECS_{t\text{-}inv}$, as shown in Fig. 2C. However, it is worth noting that even under 1396 µmol photons m^{-2} s^{-1}, the $ECS_{t\text{-}inv}$ is still 29.3 ± 5% of the ECS_t, implying a substantial Δψ contribution to *pmf* even under high light in the WT.

It is worth noting the overall 'signal drift' of the ECS kinetics recorded on the WT leaves, with the overall ECS signal rising to a maximum at around 548 µmol photons m^{-2} s^{-1}, approximately half-way through the assay. This has been proposed to be due to the overlap of the relatively slowly forming ΔA505 signal (half time 6 - 8 minutes) with the ECS (Johnson et al., 2009; Klughammer et al., 2013; Wilson and Ruban, 2020).

Disentangling the impact of xanthophyll cycle activity on the electrochromic shift signal changes

To disentangle the impact of the xanthophyll cycle on the ECS signal, *npq1*, a mutant lacking violaxanthin de-epoxidase activity was measured. This mutant is unable to synthesise zeaxanthin, and lacks the corresponding ΔA505 absorption increase (Niyogi et al., 1998; Johnson et al., 2009). Interestingly, the ECS and ΔA535 signals for *npq1* show sharp differences with respect to the WT (Fig 3A and B). Firstly, the ECS signal contains no general upward signal drift, confirming this feature is related to the ΔA505 change. Furthermore, ΔA535 absorption change in *npq1* is greatly

diminished, consistent with the fact that in the absence of zeaxanthin the qE-related absorption changes are smaller and now peak at 525 nm (Fig 1B) (Johnson et al., 2009; Ilioaia et al., 2011; Johnson and Ruban, 2014). Under light intensities lower than the growth intensity (< 190 µmol photons m^{-2} s^{-1}), there is an initial sharp rise in the ECS signal, which, after ~60 s, decays to a level slightly above the following dark pseudo-baseline, similar to WT (Fig. 3A; Fig. S1). However, in *npq1*, there is little to no upward drift in the light or downward signal drift in the dark away from the baseline. The similar levels and kinetics of the ΔA535 signal between WT and *npq1* at these low light intensities, particularly at 71 µmol photons m^{-2} s^{-1}, suggests that signal drift is therefore likely associated with zeaxanthin synthesis, and not the wavelength of the qE-related peak. At more moderate light intensities (308 – 548 µmol photons m^{-2} s^{-1}), the ECS_t again reaches its maximum. However, the balance between ECS_{inv} and $ECS_{t\text{-}inv}$ differs from the observed behaviour in WT leaves. After illumination at 548 µmol photons m^{-2} s^{-1}, the $ECS_{t\text{-}inv}$ is ~50% higher than in WT leaves ($P < 0.01$). Interestingly, there is a maintained offset of the *npq1* $ECS_{t\text{-}inv}$ of about 50% throughout the rest of the light titration, relative to the WT $ECS_{t\text{-}inv}$. According to the ECS parsing method, this would imply that in the absence of zeaxanthin, Δψ becomes the dominant component of the *pmf* under light intensities ≥ 308 µmol photons m^{-2} s^{-1} in *npq1*. Alternatively, the blue shift of the qE-related peak to 525 nm and the lack of a ΔA505 absorption change is responsible for the skewing of the ECS_{inv} and $ECS_{t\text{-}inv}$ kinetics relative to WT. It is interesting to note in *npq1* that the ECS_t follows a nearly identical relationship to light intensity as in the WT, as shown in Fig. 3C. This is in agreement with studies showing that absence of violaxanthin de-epoxidation in *npq1* has no effect on the total *pmf* amplitude or ΔpH relative to the WT (Crouchman et al., 2006; Johnson et al., 2012).

We next examined the *npq2* mutant lacking the zeaxanthin epoxidase. Since *npq2* constitutively accumulates zeaxanthin during development in place of violaxanthin, it lacks the light-induced ΔA505 (Niyogi et al., 1998; Pérez-Bueno et al., 2008; Johnson et al., 2009). Consistent with this the baseline of the ECS signal shows no upward drift during illumination cycles as seen in the WT (Fig. 4A). The qE-related ΔA535 remains in this mutant (Fig. 4B), though it is red-shifted, peaking at 540 nm (Fig. 1B; Johnson et al., 2009). If amplitude of the $ECS_{t\text{-}inv}$ signal is influenced by the degree of overlap with the qE-related absorption change then it should be affected in this mutant. In Fig. 4C, this effect is observed. At light intensities up to 151 µmol photons m^{-2} s^{-1}, the ECS signal forms a larger $ECS_{t\text{-}inv}$ component than the WT (Fig. 4A). Again similar to WT, the partitioning between the ECS_{inv} and $ECS_{t\text{-}inv}$ is approximately 1:1 at 308 µmol photons m^{-2} s^{-1} ($P > 0.05$). Interestingly, at the top three light intensities used (708, 1128, and 1396 µmol photons m^{-2} s^{-1}), the ECS_{inv} signal rises to a level where it now exceeds the ECS_t (Fig 4A & C). This effect can be explained by increased positive contribution of the qE-related absorption change (Fig. 1B; ~540 nm in *npq2*) to the 550 nm signal that is used for calculation of the ECS signal (ΔA 550 - 515 nm). The

result is that using the ECS parsing method, at light intensities ≥ 417 µmol photons m^{-2} s^{-1}, virtually all *pmf* in *npq2* is present as ΔpH (Fig. 4C).

PsbS-mediated modulation of qE and its effect on the electrochromic shift signal

The amplitude and kinetics of qE also depend on the levels of the PsbS protein, which interacts with LHCII altering its ΔpH sensitivity by promoting its aggregation (Li et al., 2002; Crouchman et al., 2006) (Johnson and Ruban, 2011; Sacharz et al., 2017). The *npq4* mutant which lacks PsbS, still displays the ΔA505 associated with zeaxanthin synthesis but lacks qE (Horton et al., 2000; Li et al., 2000). In line with this, we find the slow rise of the baseline of the ECS signal during illumination is still present in *npq4* (Fig. 5A), though the ΔA535 is greatly diminished at all light intensities measured (Fig. 5B). In line with the virtual absence of the ΔA535 signal, the $ECS_{t\text{-}inv}$ in *npq4* is smaller at light intensities ≥ 308 µmol photons m^{-2} s^{-1} compared to the WT (Fig 5A). According to the ECS parsing method at 417 µmol photons m^{-2} s^{-1}, 73.61 ± 5% of the total maximum ECS_t is present as ΔpH (ECS_{inv}) in *npq4*, versus just 50.43 ± 4% in the WT plants ($P < 0.01$). Indeed, at the maximum light intensity tested here (1396 µmol photons m^{-2} s^{-1}), the ECS_{inv} reaches 94.13 ± 6% of the ECS_t in *npq4,* compared to 70.67 ± 3% in the WT ($P < 0.01$).

To further test our hypothesis that the ECS signal is polluted by the qE-related ΔA535, we investigated the PsbS-overexpressor plants, *L17*, which show a two-fold larger qE-response compared to the WT (Li et al., 2002; Crouchman et al., 2006). Increased qE in *L17* should result in a larger ΔA535 signal and a corresponding increase in the extent of the overlap with the ECS signal. Consistent with this, ECS and ΔA535 kinetics in *L17* display stark differences compared to the WT (Fig. 6A & B). In *L17*, the ΔA535 signal is ~2.15 times that of the WT and ~10 times that of *npq4* at 1396 µmol photons m^{-2} s^{-1}. The larger amplitude of the ΔA535 signal in *L17* results in a much larger overlap with the ECS signal and therefore a much larger $ECS_{t\text{-}inv}$ signal persists at the highest light intensities used compared to the WT (Fig 6A & C). Therefore, according to the ECS parsing method, Δψ ($ECS_{t\text{-}inv}$) in *L17* comprises 77.0 ± 0.04% of the total *pmf* at 1396 µmol photons m^{-2} s^{-1} (Fig 6C), the reverse of the situation described above for *npq4* (Fig 5C).

The nature of the electrochromic shift signal in the absence of PsbS and zeaxanthin

While the $ECS_{t\text{-}inv}$ signal in *npq4* is lower than that observed in the WT under moderate and high illumination (≥ 308 µmol photons m^{-2} s^{-1}; Fig. 5C), it is still not completely absent. One possibility is that the remaining signal reflects the gradual rise of the ECS baseline due to the ΔA505 associated with zeaxanthin synthesis. To test this idea further we investigated the *npq1npq4* double mutant that lacks both zeaxanthin synthesis and qE (Li et al., 2000). In the *npq1npq4* mutant, the ECS and ΔA535 kinetics (Fig. 7A & B) display very different behaviour to WT leaves. Up to 417 µmol

photons m^{-2} s^{-1}, there appears to be a small contribution (< 10%) of $ECS_{t\text{-}inv}$ to the total ECS_t, which may reflect the true contribution of Δψ to the total *pmf*, free from overlapping ΔA505 and ΔA535 signals. However, as the ECS_t signal reaches its maxima at 308 µmol photons m^{-2} s^{-1}, the ECS_{inv} accounts for 89.7 ± 8.3 % of the total *pmf* rising to 100% above this intensity. These ECS kinetics closely match those previously reported for the *lut2npq1* mutant that also lacks both ΔA505 and ΔA535 (Johnson and Ruban 2014). Therefore, in the absence of these overlapping signals the ECS parsing method would conclude that the majority of the steady-state *pmf* is comprised of ΔpH at all light intensities measured and that any Δψ contribution to the *pmf* is dissipated within 60 seconds.

Discussion

Overlap, origin of absorption changes

Over the past 20 years, much work has been focussed on trying to measure the amplitude, kinetics and parsing of the *pmf* non-invasively in leaves using the ECS signal peaking at 515 nm (Kramer et al., 1999). This method has been widely adopted by the photosynthesis research community and has provided a useful tool for comparing the *pmf* phenotypes of a wide-range of photosynthetic mutants. Nonetheless from the inception of the ECS method it was recognised that the overlapping absorption changes associated with qE (ΔA535) and zeaxanthin formation (ΔA505) could influence the ECS signal. Since these absorption changes form and relax relatively slowly (ΔA505, minutes timescale; ΔA535, seconds to minutes timescale) they will have relatively little effect on parameters calculated from the rapid (ms) light-to-dark transition changes in the ECS signal (e.g. proton conductivity (gH^+), proton flux (vH^+) and total *pmf* (ECS_t). Indeed, the constancy of the total *pmf* across the different mutants used in this study supports this view. However, it is worth noting that rapid fluxes of ions on a ms timescale may affect the ECS signal and cause a potential underestimation of the total *pmf*. In contrast, the parsing of ECS is calculated based on the relatively slower ECS signal changes occurring in the time following the first 60 s illumination or in the 60 s following cessation of illumination where clearly the overlap presents more of an issue. Early work attributed the ΔA535 to selective light scattering, and thus Kramer and co-workers attempted to remove its contribution through pre-scattering the incident light (Kramer and Sacksteder, 1998; Cruz et al., 2001). However, later work using resonance Raman spectroscopy showed that the ΔA535 arose from a genuine absorption change and hence this approach fails (Ruban et al., 2002; Duffy et al., 2010; Ilioaia et al., 2011). Johnson and Ruban (2014) highlighted the potential extent of this overlap issue by showing that any $ECS_{t\text{-}inv}$ signal is missing from the *lut2npq1* mutant that lacks the ΔA505 and ΔA535 changes. Since *lut2npq1*chloroplasts showed identical quenching of 9-aminoacridine (9AA) fluorescence compared to the WT, this suggested that *pmf* is entirely composed of ΔpH and that the

325 $ECS_{t\text{-}inv}$ signal arises from the overlap with the ΔA505 and ΔA535 in the WT. This idea was further
326 corroborated by the fact that the $ECS_{t\text{-}inv}$ signal in the WT could be abolished with an uncoupler.
327 Nevertheless, perhaps because the Johnson and Ruban (2014) study was carried out using a mutant
328 with quite divergent carotenoid composition compared to the WT, and only at a single high light
329 intensity (700 µmol photons m^{-2} s^{-1}) where the contribution of the Δψ to the *pmf* has been argued to
330 be small (Klughammer et al., 2013), this work has been largely overlooked and the ECS parsing
331 method has remained in widespread use.

332 In the current study, we lay bare the full extent of the overlap issue across the full range of
333 light intensities from low (72 µmol photons m^{-2} s^{-1}) to high (1396 µmol photons m^{-2} s^{-1}) using a
334 wide range of Arabidopsis plants with altered ΔA535, ΔA505, or both absorption changes. From
335 our data, it is apparent that the $ECS_{t\text{-}inv}$ signal corresponds closely with the extent of ΔA535. As
336 more and more zeaxanthin is synthesised as the light intensity increases, the qE-related signal shifts
337 from 523 nm towards 535 nm and hence the extent of the overlap with the ECS signal is reduced
338 (Fig 1B) (Johnson and Ruban, 2014). Consistent with this in *npq1,* which lacks zeaxanthin, the $ECS_{t\text{-}inv}$
339 remains large under high light intensities unlike in the WT since the qE-related signal remains
340 'stuck' at 523 nm (Fig. 1B) (Johnson et al., 2009). A similar situation is seen in the PsbS
341 overexpressor *L17*, where zeaxanthin is present, but the greatly increased amplitude of the ΔA535
342 absorption change increases the extent of overlap with the ECS, resulting in a large $ECS_{t\text{-}inv}$
343 contribution, particularly at high light. Application of the ECS parsing method to these mutants
344 would suggest a greatly enhanced Δψ and diminished ΔpH contribution to the total *pmf*. If true, such
345 a large Δψ would lead to significant photoinhibition of PSII through promotion of charge
346 recombination (Bennoun, 1994; Davis et al., 2016; Davis et al., 2017). Moreover, the extremely
347 small ΔpH would preclude the formation of the large qE observed in *L17* and the normal
348 photosynthetic control observed in both (Roach and Krieger-Liszkay, 2012; Tikkanen et al., 2015).
349 Indeed, previous studies have shown that the level of 9AA quenching and so ΔpH in isolated
350 chloroplasts of *L17* is unchanged compared to the WT (Crouchman et al., 2006). Likewise, the
351 results from the *npq4* mutant highlight that when qE is inhibited by the absence of PsbS, the qE-
352 related absorption changes are largely lost and then $ECS_{t\text{-}inv}$ contribution seen in the WT is
353 accordingly greatly diminished. The residual $ECS_{t\text{-}inv}$ in *npq4* can be largely attributed to the ΔA505
354 absorption change and its elimination in the *npq1npq4* mutant allows us to see that *pmf* is
355 predominantly composed of ΔpH once the steady-state has been established via counter ion-
356 movements in the 10 - 60 s that follow illumination. Once again, the ECS parsing method would
357 suggest that ΔpH is enhanced in the *npq4* and *npq1npq4* compared to the WT, yet the photosynthetic
358 control phenotypes of these mutants confirm it is unchanged (Horton et al., 2000; Roach and
359 Krieger-Liszkay, 2012; Tikkanen et al., 2015). Our conclusion of a dominant ΔpH contribution to

pmf is in agreement with the recent theoretical model of Lyu and Lazár (2017), which suggested a steady-state Δψ of just 14 mV, which is ~10 - 15% of the total *pmf* value required to drive ATP synthesis given a H^+/ATP of 4 - 4.67, as suggested by both functional (Steigmiller et al., 2008; Petersen et al., 2012) and structural studies (Daum et al., 2010; Hahn et al., 2018). Furthermore, Lyu and Lazár (2017) show that whilst high light intensities promote *pmf* storage as ΔpH, even under low light intensities the contribution of Δψ remains small, again in agreement with the measurements here on the *npq1npq4* mutant.

How might our conclusion that *pmf* is dominated by ΔpH in both low and high light be reconciled with the work carried out in the last decade on thylakoid ion channels? To date, three classes of thylakoid ion channels have been reported, the TPK3 K^+ transporter (Carraretto et al., 2013), the VCCN1 Cl^- transporter (Duan et al., 2016; Herdean et al., 2016a; Herdean et al., 2016b) and the KEA3 H^+/K^+ antiporter (Armbruster et al., 2014). The partial absence of counterion channels in the thylakoid would be anticipated to alter the WT situation, where ΔpH dominates, leaving a larger Δψ that would diminish qE. Indeed, the *vccn1* and *tpk3* mutants show lower qE and an increase in $ECS_{t\text{-}inv}$, while the extent of total *pmf* is similar (Carraretto et al., 2013; Herdean et al., 2016a; Herdean et al., 2016b). In contrast, overexpressors of VCCN1 (oeVCCN1) show a complete absence of $ECS_{t\text{-}inv}$, and therefore 100% ΔpH, which the authors used as an argument for the existence of a steady-state Δψ component in the WT (Herdean et al., 2016b). However, the oeVCCN1 plants also showed an increase in the total *pmf* and zeaxanthin synthesis, both of which reduce the overlap of qE-related absorption changes with the ECS as seen here for *npq2*, and in our previous study (Johnson and Ruban, 2014). Plants lacking KEA3 (*kea3*) show slower recovery from qE upon dark-to-low light or high light–to-low light transitions, and a corresponding penalty in terms of PSII efficiency and CO_2 fixation (Armbruster et al., 2014; Armbruster et al., 2016). $ECS_{t\text{-}inv}$ is decreased in *kea3* compared to the WT suggesting some steady-state Δψ in the latter. However, the lower $ECS_{t\text{-}inv}$ could also be explained by reduced overlap between ΔA535 and the ECS due to increased zeaxanthin formation in *kea3* (Armbruster et al., 2014; Armbruster et al., 2016). Upon high-to-low transitions in light intensity, a sudden drop in proton-coupled electron transfer, but continued H^+ efflux through the ATPase leads to a transient inverse Δψ (Kramer et al., 2003). The inverted field limits the rate of H^+ efflux and therefore qE relaxation, thus, an electroneutral antiporter, such as KEA3, would allow more rapid dissipation of *pmf* than would be possible by the ATPase alone. The slower counterion movements would then subsequently restore the steady-state domination of ΔpH at a new lower level of *pmf*. To our knowledge, Arabidopsis mutants lacking Ca^{2+}/H^+ or Mg^{2+}/H^+ antiporters are yet to be generated and characterised, despite evidence of both being identified in the thylakoid membrane (Barber et al., 1974; Ettinger et al., 1999). In the future,

crossing the ion-channel mutants into the *npq1npq4* background has the potential to clarify their net contributions to the dissipation of $\Delta\psi$ in the steady-state.

Domination of *pmf* in low and high light by the ΔpH and its apparent saturation at 308 µmol photons m^{-2} s^{-1} in the *npq1npq4* mutant raises a series of interesting issues for the regulation of photosynthesis. If *pmf* is saturated at moderate light (between 308 and 548 µmol photons m^{-2} s^{-1}) in the WT (Fig. 2C), why then is qE (and ΔA535) still seen to increase gradually up to the maximum light intensity used of 1396 (Fig. 2B)? A similar early saturation of ΔpH formation is observed in isolated chloroplasts using 9AA (Schuldiner et al., 1972; Oxborough and Horton, 1988; Ruban and Horton, 1999; Evron and McCarty, 2000; Johnson and Ruban, 2011; Roach and Krieger-Liszkay, 2012; Johnson and Ruban, 2014; Yamamoto and Shikanai, 2020). This discrepancy can be explained by the relatively slow synthesis of zeaxanthin, which shows a half-time of ~6 – 8 minutes under high illumination (Bilger et al., 1989; Johnson et al., 2009; Townsend et al., 2018; Wilson and Ruban, 2020). Thus, despite the saturation of pmf at moderate light, qE continues to increase since de-epoxidation of violaxanthin to zeaxanthin shifts the pKa of the qE response from ~5.0 to 6.0 (Horton et al., 1991; Horton et al., 2000; Ruban et al., 2012). This type of allosteric control is particularly crucial since it allows maximal rates of LET and qE to co-exist. Similar to qE, measurements of photosynthetic control, using the proxy of $P700^+$ accumulation, suggest it reaches a maximum at high rather than moderate light intensities (Suorsa et al., 2013). However, there is evidence that photosynthetic control is also regulated by the redox state of the $NADP^+$/NADPH pool, with reducing conditions increasing pH sensitivity of the cytb_6f complex (Johnson, 2003; Hald et al., 2008). Redox regulation may therefore work synergistically with ΔpH to regulate photosynthetic control as the xanthophyll cycle regulates qE. Such complex regulation of photosynthesis is necessary because, otherwise, the excessively large ΔpH that would be required to give the requisite downregulation of cytb_6f, and increase in qE, would lead to the inhibition of the oxygen-evolving complex of PSII (Krieger and Weis, 1993; Spetea et al., 1997; Zaharieva et al., 2011; Wilson and Ruban, 2019).

Conclusion

Our data show that the slow secondary rise of the ECS signal during illumination in the WT is caused by the strongly overlapping absorption changes associated with zeaxanthin synthesis and qE. In Arabidopsis mutants lacking an active xanthophyll cycle or qE activity, where ΔA505 and ΔA535 signals are absent it is clear that the $\Delta\psi$ component of the *pmf* is dissipated almost completely (< 10% contribution) within 60 s of illumination. The data here are therefore in agreement with the wide range of existing experimental data in the literature derived from microelectrodes, pH sensitive dyes, and radiolabelling experiments (Dilley and Vernon, 1965; Bulychev et al., 1972; Rottenberg

et al., 1972; Schuldiner et al., 1972; Barber et al., 1974; Pick et al., 1974; Chow et al., 1976; Vredenberg and Bulychev, 1976; Slovacek and Hind, 1981; Bulychev, 1984; Van Kooten et al., 1986; Remiš et al., 1986; Vredenberg, 1997) all of which show a dominant ΔpH contribution to *pmf* in both low and high light.

Materials and methods

Plant growth conditions

Wild-type (WT) Arabidopsis (*Arabidopsis thaliana*) (Col-0), the violaxanthin de-epoxidase knockout (*npq1*; Niyogi et al., 1998), the PsbS knockout (*npq4*; Li et al., 2000), the PsbS overexpressor (*L17*; Li et al., 2002), and the violaxanthin de-epoxidase and PsbS double-knockout mutant (*npq1npq4*; Havaux and Niyogi, 1999) were used in this study. Seeds were sterilised in 50% (v/v) ethanol and 0.1% (v/v) Triton-X 100 and were stored for 48 h at 4 °C before being sown on a 6:6:1 ratio of Levington M3 compost, John Innes No. 3 soil, and Perlite (Scotts U.K., Ipswich, U.K.). All measurements were carried out on 4-5-week-old plants, grown at 190 µmol photons m^{-2} s^{-1} with a 10-hour photoperiod at 22 °C. Plants were grown in a Percival AR-75L3 plant growth cabinet (Percival Scientific Inc., U.S.A.), equipped with Phillips MASTER TL-D Super 80 36 W/840 bulbs, which emit a cool white light (Koninklijke Philips N.V., Netherlands). Before each measurement, plants were dark adapted for 30 min.

Absorption measurements in leaves

Electrochromic shift and 535 nm absorption kinetics were measured in parallel on attached leaves on a Walz DUAL-PAM-100 (Walz, Germany) and its P515/535 emitter-detector modules (Schreiber and Klughammer, 2008), with the measuring light set to a frequency of 1000 Hz. To calibrate each measurement to account for varying leaf thickness and chlorophyll content, the ECS signal wavelengths (ΔA 550 – 515 nm) were balanced using the inbuilt software and the ECS kinetics from a single-turnover pulse. Leaves were illuminated for 3 min, followed by 3 min darkness over a total of 8 steps of increasing red actinic light (λ = 635 nm). The actinic light intensities used were 0, 71, 151, 308, 417, 548, 708, 1128, 1396 µmol photons m^{-2} s^{-1}. ECS_t, ECS_{inv}, and $ECS_{t\text{-}inv}$ were calculated as previously described (Sacksteder and Kramer, 2000; Klughammer et al., 2013), and as shown in Fig. 1C.

Absorption spectra in the 410-560 nm region were measured using a SLM DW2000 dual wavelength spectrophotometer (Olis Inc., U.S.A.), as previously described (Johnson et al., 2009). Whole Arabidopsis leaves were detached from plants dark-adapted for 30 min and the petioles wrapped in moist filter paper. The leaves were inserted into a $1cm^2$ transparent cuvette at 45º to the DW2000 measuring light path. An optic fiber, at 90° to the DW2000 measuring light, delivered red actinic light (700 µmol photons m^{-2} s^{-1}) illuminating the leaf at 45º, and was defined using a Corning 2-58 filter. The photomultiplier was protected using a Corning 4-96 filter and an OCLl Cyan T400-570

mirror. The instrument slit-width was 5 nm and the scan rate was 4 nm s^{-1}. The sample compartment was water-cooled to maintain the leaf temperature at 22ºC.

Accession numbers

The sequence data from this article can be found in The Arabidopsis Information Resource database (https://www.arabidopsis.org/) under the following accession numbers: *npq1* (AT1G08550); *npq4/L17* (AT1G44575).

Supplemental Data

Supplemental Figure S1. Expanded view of low and high illumination effect on the ECS signal in each plant line.

Acknowledgements

This work was supported by Office of The Royal Society Wolfson Research Merit Award (WM140084), a BBSRC grant [BB/L019027/1] to A.V.R. M.P.J. acknowledges funding from the Leverhulme Trust grant RPG-2019-045.

Figure legends

Fig. 1 Difference spectra and the light-to-dark transition in the electrochromic shift signal.
(A) Difference spectra of qE (black) 5 min light-*minus*-5 min dark recovery; zeaxanthin synthesis (red) dark adaptation-*minus*-5 min light; ECS (blue) 15 s light-*minus*-5 min dark recovery.
(B) qE spectra (5 min light-*minus*-5 min dark recovery) for a range of Arabidopsis transformants. WT (black); *npq1* (blue); *npq2* (red); *L17* (grey).
(C) ECS kinetic signal (ΔA 550 – 515 nm) measured on a WT Arabidopsis leaf. The magnitude of the trough formed upon cessation of illumination is the ECS_t. The difference between the minima of the ECS_t and the steady-state signal in the dark is termed the ECS_{inv}. Thus, the difference between ECS_t and ECS_{inv} is termed the $ECS_{t\text{-}inv}$.
ECS, electrochromic shift; AL, actinic light.

Fig. 2 Electrochromic shift and 535 nm measurements on WT leaves. (A) Representative ECS (ΔA 550 – 515 nm) and (B) ΔA 535 nm kinetics. Each assay consisted of 8 steps of 3 min illumination (white bars) and 3 min darkness (black bars). The illumination increased at each step using 0, 71, 151, 308, 417, 548, 708, 1128, and 1396 µmol photons m^{-2} s^{-1}. (C) ECS_t, ECS_{inv}, and $ECS_{t\text{-}inv}$ at each light intensity. Here, measurements are normalised to the maximum ECS_t. Error bars represent SEM (n = 7). ECS, electrochromic shift.

Fig. 3 Electrochromic shift and 535 nm measurements on *npq1* leaves. (A) Representative ECS (ΔA 550 – 515 nm) and (B) ΔA 535 nm kinetics. Each assay consisted of 8 steps of 3 min illumination (white bars) and 3 min darkness (black bars). The illumination increased at each step using 0, 71, 151, 308, 417, 548, 708, 1128, and 1396 µmol photons m^{-2} s^{-1}. (C) ECS_t, ECS_{inv}, and $ECS_{t\text{-}inv}$ at each light intensity. Here, measurements are normalised to the maximum ECS_t. Error bars represent SEM (n = 8). ECS, electrochromic shift.

Fig. 4 Electrochromic shift and 535 nm measurements on *npq2* leaves. (A) Representative ECS (ΔA 550 – 515 nm) and (B) ΔA 535 nm kinetics. Each assay consisted of 8 steps of 3 min illumination (white bars) and 3 min darkness (black bars). The illumination increased at each step using 0, 71, 151, 308, 417, 548, 708, 1128, and 1396 µmol photons m^{-2} s^{-1}. (C) ECS_t, ECS_{inv}, and $ECS_{t\text{-}inv}$ at each light intensity. Here, measurements are normalised to the maximum ECS_t. Error bars represent SEM (n = 6). ECS, electrochromic shift.

Fig. 5 Electrochromic shift and 535 nm measurements on *npq4* leaves. (A) Representative ECS (ΔA 550 – 515 nm) and (B) ΔA 535 nm kinetics. Each assay consisted of 8 steps of 3 min illumination (white bars) and 3 min darkness (black bars). The illumination increased at each step using 0, 71, 151, 308, 417, 548, 708, 1128, and 1396 µmol photons m^{-2} s^{-1}. (C) ECS_t, ECS_{inv}, and $ECS_{t\text{-}inv}$ at each light intensity. Here, measurements are normalised to the maximum ECS_t. Error bars represent SEM (n = 8). ECS, electrochromic shift.

Fig. 6 Electrochromic shift and 535 nm measurements on *L17* leaves. (A) Representative ECS (ΔA 550 – 515 nm) and (B) ΔA 535 nm kinetics. Each assay consisted of 8 steps of 3 min illumination (white bars) and 3 min darkness (black bars). The illumination increased at each step using 0, 71, 151, 308, 417, 548, 708, 1128, and 1396 µmol photons m^{-2} s^{-1}. (C) ECS_t, ECS_{inv}, and $ECS_{t\text{-}inv}$ at each light intensity. Here, measurements are normalised to the maximum ECS_t. Error bars represent SEM (n = 8). ECS, electrochromic shift.

Fig. 7 Electrochromic shift and 535 nm measurements on *npq1npq4* leaves. (A) Representative ECS (ΔA 550 – 515 nm) and (B) ΔA 535 nm kinetics. Each assay consisted of 8 steps of 3 min illumination (white bars) and 3 min darkness (black bars). The illumination increased at each step using 0, 71, 151, 308, 417, 548, 708, 1128, and 1396 µmol photons m^{-2} s^{-1}. (C) ECS_t, ECS_{inv}, and $ECS_{t\text{-}inv}$ at each light intensity. Here, measurements are normalised to the maximum ECS_t. Error bars represent SEM (n = 5).

References

Armbruster U, Carrillo LR, Venema K, Pavlovic L, Schmidtmann E, Kornfeld A, Jahns P, Berry JA, Kramer DM, Jonikas MC (2014) Ion antiport accelerates photosynthetic acclimation in fluctuating light environments. Nat Commun **5**: 1–8

Armbruster U, Correa Galvis V, Kunz HH, Strand DD (2017) The regulation of the chloroplast proton motive force plays a key role for photosynthesis in fluctuating light. Curr Opin Plant Biol **37**: 56–62

Armbruster U, Leonelli L, Galvis VC, Strand D, Quinn EH, Jonikas MC, Niyogi KK (2016) Regulation and levels of the thylakoid K+/H+ antiporter KEA3 shape the dynamic response of photosynthesis in fluctuating light. Plant Cell Physiol. doi: 10.1093/pcp/pcw085

Bailleul B, Cardol P, Breyton C, Finazzi G (2010) Electrochromism: A useful probe to study algal photosynthesis. Photosynth Res **106**: 179–189

Barber J, Mills J, Nicolson J (1974) Studies with cation specific ionophores show that within the intact chloroplast Mg++ acts as the main exchange cation for H + pumping. FEBS Lett **49**: 106–110

Bennoun P (1994) Chlororespiration revisited: Mitochondrial-plastid interactions in Chlamydomonas. BBA - Bioenerg **1186**: 59–66

Bilger W, Björkman O (1990) Role of the xanthophyll cycle in photoprotection elucidated by measurements of light-induced absorbance changes, fluorescence and photosynthesis in leaves of Hedera canariensis. Photosynth Res **25**: 173–185

Bilger W, Bjorkman O, Thayer SS (1989) Light-Induced Spectral Absorbance Changes in Relation to Photosynthesis and the Epoxidation State of Xanthophyll Cycle Components in Cotton Leaves. Plant Physiol **91**: 542–551

Bulychev AA (1984) Different kinetics of membrane potential formation in dark-adapted and preilluminated chloroplasts. Biochim Biophys Acta - Bioenerg **766**: 647–652

Bulychev AA, Andrianov VK, Kurella GA, Litvin FF (1972) Micro-electrode Measurements of the transmembrane potential of chloroplasts and its photoinduced changes. Nature **236**: 175–177

Carraretto L, Formentin E, Teardo E, Checchetto V, Tomizioli M, Morosinotto T, Giacometti GM, Finazzi G, Szabó I (2013) A Thylakoid-Located Two-Pore K + Channel Controls Photosynthetic Light Utilization in Plants. Science (80-) **342**: 114–118

561 **Chow W, Wagner A, Hope A** (1976) Light-dependent Redistribution of Ions in Isolated Spinach
562 Chloroplasts. Funct Plant Biol **3**: 853

563 **Crouchman S, Ruban A, Horton P** (2006) PsbS enhances nonphotochemical fluorescence
564 quenching in the absence of zeaxanthin. FEBS Lett **580**: 2053–2058

565 **Cruz JA, Sacksteder CA, Kanazawa A, Kramer DM** (2001) Contribution of Electric Field (Δψ)
566 to Steady-State Transthylakoid Proton Motive Force (pmf) in Vitro and in Vivo. Control of
567 pmf Parsing into Δψ and ΔpH by Ionic Strength. Biochemistry **40**: 1226–1237

568 **Daum B, Nicastro D, Austin J, McIntosh JR, Kühlbrandt W** (2010) Arrangement of
569 Photosystem II and ATP Synthase in Chloroplast Membranes of Spinach and Pea. Plant Cell
570 **22**: 1299–1312

571 **Davis GA, Kanazawa A, Schöttler MA, Kohzuma K, Froehlich JE, William Rutherford A,**
572 **Satoh-Cruz M, Minhas D, Tietz S, Dhingra A, et al** (2016) Limitations to photosynthesis
573 by proton motive force-induced photosystem II photodamage. Elife **5**: 23–27

574 **Davis GA, Rutherford AW, Kramer DM** (2017) Hacking the thylakoid proton motive force for
575 improved photosynthesis: Modulating ion flux rates that control proton motive force
576 partitioning into ΔΨ and ΔpH. Philos Trans R Soc B Biol Sci **372**: 20160381

577 **Dilley RA, Vernon LP** (1965) Ion and water transport processes related to the light-dependent
578 shrinkage of spinach chloroplasts. Arch Biochem Biophys **111**: 365–375

579 **Duan Z, Kong F, Zhang L, Li W, Zhang J, Peng L** (2016) A bestrophin-like protein modulates
580 the proton motive force across the thylakoid membrane in Arabidopsis. J Integr Plant Biol
581 **58**: 848–858

582 **Duffy CDP, Johnson MP, Macernis M, Valkunas L, Barford W, Ruban A V.** (2010) A
583 theoretical investigation of the photophysical consequences of major plant light-harvesting
584 complex aggregation within the photosynthetic membrane. J Phys Chem B **114**: 15244–
585 15253

586 **Duniec JT, Thorne SW** (1977) The relation of light-induced slow absorbancy and scattering
587 changes about 520 nm and structure of chloroplast thylakoids-A theoretical investigation. J
588 Bioenerg Biomembr **9**: 223–235

589 **Ettinger WF, Clear AM, Fanning KJ, Peck M Lou** (1999) Identification of a Ca2+/H+ Antiport
590 in the Plant Chloroplast Thylakoid Membrane. Plant Physiol **119**: 1379–1386

591 **Evron Y, McCarty RE** (2000) Simultaneous Measurement of ΔpH and Electron Transport in

592 Chloroplast Thylakoids by 9-Aminoacridine Fluorescence. Plant Physiol **124**: 407–414

593 **Hahn A, Vonck J, Mills DJ, Meier T, Kühlbrandt W** (2018) Structure, mechanism, and
594 regulation of the chloroplast ATP synthase. Science (80-) **360**: eaat4318

595 **Hald S, Nandha B, Gallois P, Johnson GN** (2008) Feedback regulation of photosynthetic
596 electron transport by NADP(H) redox poise. Biochim Biophys Acta - Bioenerg **1777**: 433–
597 440

598 **Hangarter RP, Good NE** (1982) Energy thresholds for ATP synthesis in chloroplasts. Biochim
599 Biophys Acta - Bioenerg **681**: 397–404

600 **Havaux M, Niyogi KK** (1999) The violaxanthin cycle protects plants from photooxidative
601 damage by more than one mechanism. Proc Natl Acad Sci **96**: 8762–8767

602 **Herdean A, Nziengui H, Zsiros O, Solymosi K, Garab G, Lundin B, Spetea C** (2016a) The
603 Arabidopsis thylakoid chloride channel AtCLCe functions in chloride homeostasis and
604 regulation of photosynthetic electron transport. Front Plant Sci **7**: 1–15

605 **Herdean A, Teardo E, Nilsson AK, Pfeil BE, Johansson ON, Ünnep R, Nagy G, Zsiros O,**
606 **Dana S, Solymosi K, et al** (2016b) A voltage-dependent chloride channel fine-tunes
607 photosynthesis in plants. Nat Commun **7**: 1–11

608 **Horton P, Ruban A V., Rees D, Pascal AA, Noctor G, Young AJ** (1991) Control of the light-
609 harvesting function of chloroplast membranes by aggregation of the LHCII chlorophyll-
610 protein complex. FEBS Lett **292**: 1–4

611 **Horton P, Ruban A V., Wentworth M** (2000) Allosteric regulation of the light-harvesting
612 system of photosystem II. Philos Trans R Soc B Biol Sci **355**: 1361–1370

613 **Ilioaia C, Johnson MP, Duffy CDP, Pascal AA, Van Grondelle R, Robert B, Ruban A V.**
614 (2011) Origin of absorption changes associated with photoprotective energy dissipation in the
615 absence of zeaxanthin. J Biol Chem **286**: 91–98

616 **Johnson GN** (2003) Thiol regulation of the thylakoid electron transport chain - A missing link in
617 the regulation of photosynthesis? Biochemistry **42**: 3040–3044

618 **Johnson MP, Perez-Bueno ML, Zia A, Horton P, Ruban A V.** (2009) The Zeaxanthin-
619 Independent and Zeaxanthin-Dependent qE Components of Nonphotochemical Quenching
620 Involve Common Conformational Changes within the Photosystem II Antenna in
621 Arabidopsis. Plant Physiol **149**: 1061–1075

Johnson MP, Ruban A V. (2014) Rethinking the existence of a steady-state Δψ component of the proton motive force across plant thylakoid membranes. Photosynth Res **119**: 233–242

Johnson MP, Ruban A V. (2009) Arabidopsis plants lacking PsbS protein possess photoprotective energy dissipation. Plant J **61**: 283–289

Johnson MP, Ruban A V. (2011) Restoration of rapidly reversible photoprotective energy dissipation in the absence of PsbS protein by enhanced ΔpH. J Biol Chem **286**: 19973–19981

Johnson MP, Zia A, Ruban A V. (2012) Elevated ΔpH restores rapidly reversible photoprotective energy dissipation in Arabidopsis chloroplasts deficient in lutein and xanthophyll cycle activity. Planta **235**: 193–204

Kanazawa A, Kramer DM (2002) In vivo modulation of nonphotochemical exciton quenching (NPQ) by regulation of the chloroplast ATP synthase. Proc Natl Acad Sci **99**: 12789–12794

Klughammer C, Siebke K, Schreiber U (2013) Continuous ECS-indicated recording of the proton-motive charge flux in leaves. Photosynth Res **117**: 471–487

Van Kooten O, Snel JFH, Vredenberg WJ (1986) Photosynthetic free energy transduction related to the electric potential changes across the thylakoid membrane. Photosynth Res **9**: 211–227

Kramer DM, Cruz JA, Kanazawa A (2003) Balancing the central roles of the thylakoid proton gradient. Trends Plant Sci **8**: 27–32

Kramer DM, Sacksteder CA (1998) A diffused-optics flash kinetic spectrophotometer (DOFS) for measurements of absorbance changes in intact plants in the steady-state. Photosynth Res **56**: 103–112

Kramer DM, Sacksteder CA, Cruz JA (1999) How acidic is the lumen? Photosynth Res **60**: 151–163

Krieger A, Weis E (1993) The role of calcium in the pH-dependent control of Photosystem II. Photosynth Res **37**: 117–130

Lambert AJ, Brand MD (2004) Superoxide production by NADH:ubiquinone oxidoreductase (complex I) depends on the pH gradient across the mitochondrial inner membrane. Biochem J **382**: 511–517

Li X-P, Björkman O, Shih C, Grossman AR, Rosenquist M, Jansson S, Niyogi KK (2000) A pigment-binding protein essential for regulation of photosynthetic light harvesting. Nature

652 **403**: 391–395

653 **Li X-P, Müller-Moulé P, Gilmore AM, Niyogi KK** (2002) PsbS-dependent enhancement of
654 feedback de-excitation protects photosystem II from photoinhibition. Proc Natl Acad Sci **99**:
655 15222–15227

656 **Lyu H, Lazár D** (2017) Modeling the light-induced electric potential difference (ΔΨ), the pH
657 difference (ΔpH) and the proton motive force across the thylakoid membrane in C3 leaves. J
658 Theor Biol **413**: 11–23

659 **Malone LA, Proctor MS, Hitchcock A, Hunter CN, Johnson MP** (2021) Cytochrome b6f –
660 Orchestrator of photosynthetic electron transfer. Biochim Biophys Acta - Bioenerg **1862**:
661 148380

662 **Metzger SU, Cramer WA, Whitmarsh J** (1997) Critical analysis of the extinction coefficient of
663 chloroplast cytochrome f. Biochim Biophys Acta - Bioenerg **1319**: 233–241

664 **Mitchell P** (1961) Coupling of phosphorylation to electron and hydrogen transfer by a chemi-
665 osmotic type of mechanism. Nature **191**: 144–148

666 **Mitchell P** (2011) Chemiosmotic coupling in oxidative and photosynthetic phosphorylation.
667 Biochim Biophys Acta - Bioenerg **1807**: 1507–1538

668 **Murakami S, Packer L** (1970a) Light-induced Changes in the Conformation and Configuration
669 of the Thylakoid Membrane of Ulva and Porphyra Chloroplasts in Vivo. Plant Physiol **45**:
670 289–299

671 **Murakami S, Packer L** (1970b) Protonation and chloroplast membrane structure. J Cell Biol **47**:
672 332–51

673 **Nelson N, Junge W** (2015) Structure and Energy Transfer in Photosystems of Oxygenic
674 Photosynthesis. Annu Rev Biochem **84**: 659–683

675 **Nishio JN, Whitmarsh J** (1993) Dissipation of the proton electrochemical potential in intact
676 chloroplasts: II. The pH gradient monitored by cytochrome f reduction kinetics. Plant Physiol
677 **101**: 89–96

678 **Niyogi KK, Grossman AR, Björkman O** (1998) Arabidopsis Mutants Define a Central Role for
679 the Xanthophyll Cycle in the Regulation of Photosynthetic Energy Conversion. Plant Cell **10**:
680 1121–1134

681 **Oxborough K, Horton P** (1988) A study of the regulation and function of energy-dependent

682 quenching in pea chloroplasts. Biochim Biophys Acta - Bioenerg **934**: 135–143

683 **Pérez-Bueno ML, Johnson MP, Zia A, Ruban A V., Horton P** (2008) The Lhcb protein and
684 xanthophyll composition of the light harvesting antenna controls the ΔpH-dependency of
685 non-photochemical quenching in Arabidopsis thaliana. FEBS Lett **582**: 1477–1482

686 **Petersen J, Forster K, Turina P, Graber P** (2012) Comparison of the H+/ATP ratios of the H+-
687 ATP synthases from yeast and from chloroplast. Proc Natl Acad Sci **109**: 11150–11155

688 **Pick U, Rottenberg H, Avron M** (1974) The dependence of photophosphorylation in chloroplasts
689 on ΔpH and external pH. FEBS Lett **48**: 32–36

690 **Remiš D, Bulychev AA, Kurella GA** (1986) The electrical and chemical components of the
691 protonmotive force in chloroplasts as measured with capillary and pH-sensitive
692 microelectrodes. Biochim Biophys Acta - Bioenerg **852**: 68–73

693 **Roach T, Krieger-Liszkay A** (2012) The role of the PsbS protein in the protection of
694 photosystems I and II against high light in Arabidopsis thaliana. Biochim Biophys Acta -
695 Bioenerg **1817**: 2158–2165

696 **Rottenberg H, Grunwald T, Avron M** (1972) Determination of ΔpH in Chloroplasts. 1.
697 Distribution of [14C]Methylamine. Eur J Biochem **25**: 54–63

698 **Ruban A V., Horton P** (1999) The Xanthophyll Cycle Modulates the Kinetics of
699 Nonphotochemical Energy Dissipation in Isolated Light-Harvesting Complexes, Intact
700 Chloroplasts, and Leaves of Spinach. Plant Physiol **119**: 531–542

701 **Ruban A V., Johnson MP, Duffy CDP** (2012) The photoprotective molecular switch in the
702 photosystem II antenna. Biochim Biophys Acta - Bioenerg **1817**: 167–181

703 **Ruban A V., Pascal AA, Robert B, Horton P** (2002) Activation of zeaxanthin is an obligatory
704 event in the regulation of photosynthetic light harvesting. J Biol Chem **277**: 7785–7789

705 **Ruban A V, Wilson S** (2020) The Mechanism of Non-Photochemical Quenching in Plants:
706 Localization and Driving Forces. Plant Cell Physiol **44**: 1–10

707 **Sacharz J, Giovagnetti V, Ungerer P, Mastroianni G, Ruban A V.** (2017) The xanthophyll
708 cycle affects reversible interactions between PsbS and light-harvesting complex II to control
709 non-photochemical quenching. Nat Plants **3**: 1–9

710 **Sacksteder CA, Kramer DM** (2000) Dark-interval relaxation kinetics (DIRK) of absorbance
711 changes as a quantitative probe of steady-state electron transfer. Photosynth Res **66**: 145–158

Schreiber U, Klughammer C (2008) New accessory for the DUAL-PAM-100: The P515/535 module and examples of its application. PAM Appl Notes **10**: 1–10

Schuldiner S, Rottenberg H, Avron M (1972) Determination of ΔpH in Chloroplasts. 2. Fluorescent Amines as a Probe for the Determination of ΔpH in Chloroplasts. Eur J Biochem **25**: 64–70

Slovacek RE, Hind G (1981) Correlation between photosynthesis and the transthylakoid proton gradient. Biochim Biophys Acta - Bioenerg **635**: 393–404

Spetea C, Hideg É, Vass I (1997) Low pH accelerates light-induced damage of photosystem II by enhancing the probability of the donor-side mechanism of photoinhibition. Biochim Biophys Acta - Bioenerg **1318**: 275–283

Steigmiller S, Turina P, Graber P (2008) The thermodynamic H+/ATP ratios of the H+-ATPsynthases from chloroplasts and Escherichia coli. Proc Natl Acad Sci **105**: 3745–3750

Suorsa M, Grieco M, Järvi S, Gollan PJ, Kangasjärvi S, Tikkanen M, Aro EM (2013) PGR5 ensures photosynthetic control to safeguard photosystem I under fluctuating light conditions. Plant Signal Behav **8**: 167–172

Takizawa K, Cruz JA, Kanazawa A, Kramer DM (2007) The thylakoid proton motive force in vivo. Quantitative, non-invasive probes, energetics, and regulatory consequences of light-induced pmf. Biochim Biophys Acta - Bioenerg **1767**: 1233–1244

Tikkanen M, Rantala S, Aro EM (2015) Electron flow from PSII to PSI under high light is controlled by PGR5 but not by PSBS. Front Plant Sci **6**: 1–6

Townsend AJ, Saccon F, Giovagnetti V, Wilson S, Ungerer P, Ruban A V. (2018) The causes of altered chlorophyll fluorescence quenching induction in the Arabidopsis mutant lacking all minor antenna complexes. Biochim Biophys Acta - Bioenerg **1859**: 666–675

Vredenberg WJ (1997) Electrogenesis in the photosynthetic membrane: Fields, facts and features. Bioelectrochemistry Bioenerg **44**: 1–11

Vredenberg WJ, Bulychev AA (1976) Changes in the electrical potential across the thylakoid membranes of illuminated intact chloroplasts in the presence of membrane-modifying agents. Plant Sci Lett **7**: 101–107

Wilson S, Ruban A V. (2020) Enhanced NPQ affects long-term acclimation in the spring ephemeral Berteroa incana. Biochim Biophys Acta - Bioenerg **1861**: 148014

Wilson S, Ruban A V. (2019) Quantitative assessment of the high-light tolerance in plants with an impaired photosystem II donor side. Biochem J **476**: 1377–1386

Witt HT (1971) Coupling of quanta, electrons, field ions and phosphorylation in the functional membrane of photosynthesis. Quart Res Biophys **4**: 365–477

Witt HT (1979) Energy conversion in the functional membrane of photosynthesis. Analysis by light pulse and electric pulse methods. Biochim Biophys Acta - Rev Bioenerg **505**: 355–427

Wolf DM, Segawa M, Kondadi AK, Anand R, Bailey ST, Reichert AS, Bliek AM, Shackelford DB, Liesa M, Shirihai OS (2019) Individual cristae within the same mitochondrion display different membrane potentials and are functionally independent. EMBO J **38**: 1–21

Yamamoto H, Shikanai T (2020) Does the Arabidopsis proton gradient regulation5 Mutant Leak Protons from the Thylakoid Membrane? Plant Physiol **184**: 421–427

Yamamoto HY, Wang Y, Kamite L (1971) A chloroplast absorbance change from violaxanthin de-epoxidation. A possible component of 515 nm changes. Biochem Biophys Res Commun **42**: 37–42

Zaharieva I, Wichmann JM, Dau H (2011) Thermodynamic limitations of photosynthetic water oxidation at high proton concentrations. J Biol Chem **286**: 18222–18228

Wilson et al.
Fig. 1

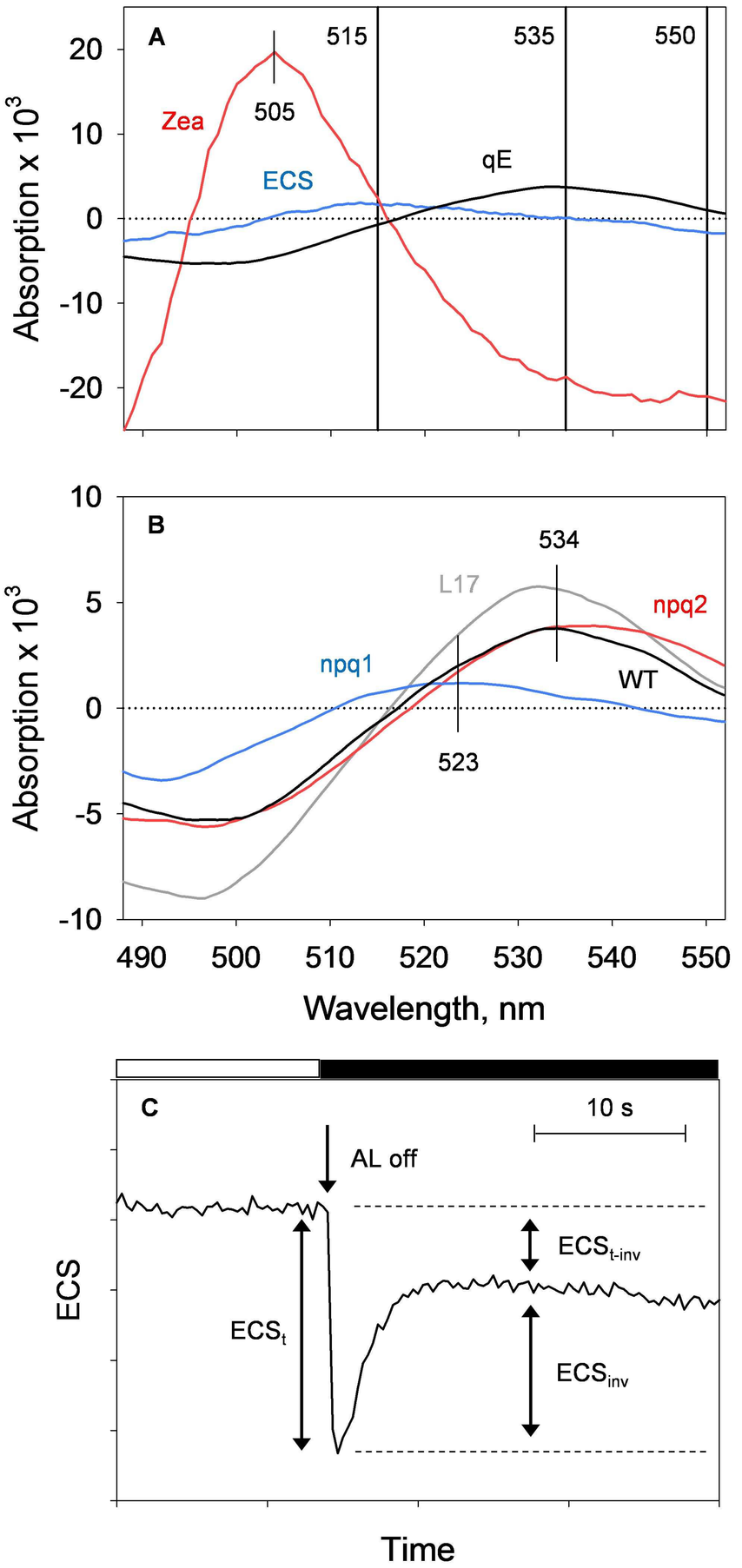

Fig. 1 Difference spectra and the light-to-dark transition in the electrochromic shift signal.

(A) Difference spectra of qE (black) 5 min light-*minus*-5 min dark recovery; zeaxanthin synthesis (red) dark adaptation-*minus*-5 min light; ECS (blue) 15 s light-*minus*-5 min dark recovery.

(B) qE spectra (5 min light-*minus*-5 min dark recovery) for a range of Arabidopsis transformants. WT (black); *npq1* (blue); *npq2* (red); *L17* (grey).

(C) ECS kinetic signal (ΔA 550 – 515 nm) measured on a WT Arabidopsis leaf. The magnitude of the trough formed upon cessation of illumination is the ECS_t. The difference between the minima of the ECS_t and the steady-state signal in the dark is termed the ECS_{inv}. Thus, the difference between ECS_t and ECS_{inv} is termed the $ECS_{t\text{-}inv}$.

ECS, electrochromic shift; AL, actinic light.

Wilson et al.
Fig. 2

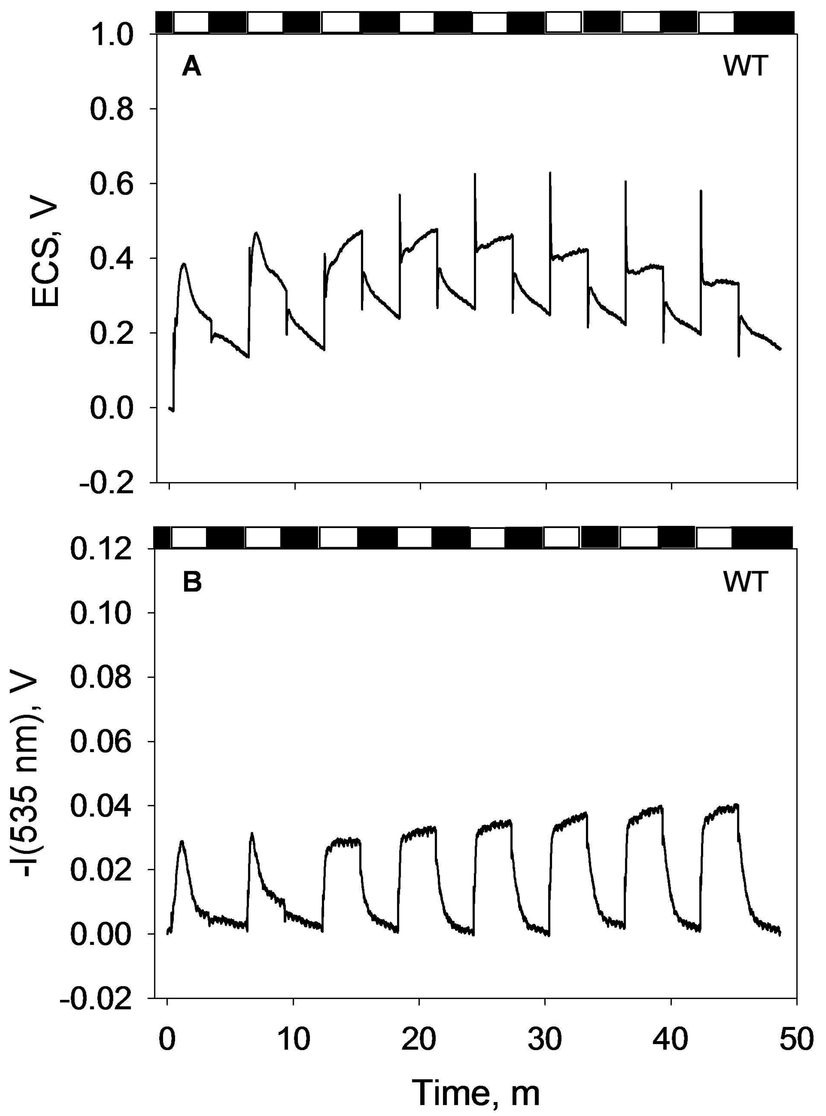

Fig. 2 Electrochromic shift and 535 nm measurements on WT leaves. (A) Representative ECS (ΔA 550 – 515 nm) and (B) ΔA 535 nm kinetics. Each assay consisted of 8 steps of 3 min illumination (white bars) and 3 min darkness (black bars). The illumination increased at each step using 0, 71, 151, 308, 417, 548, 708, 1128, and 1396 µmol photons m^{-2} s^{-1}. (C) ECS_t, ECS_{inv}, and $ECS_{t\text{-}inv}$ at each light intensity. Here, measurements are normalised to the maximum ECS_t. Error bars represent SEM (*n* = 7). ECS, electrochromic shift.

Wilson et al.
Fig. 3

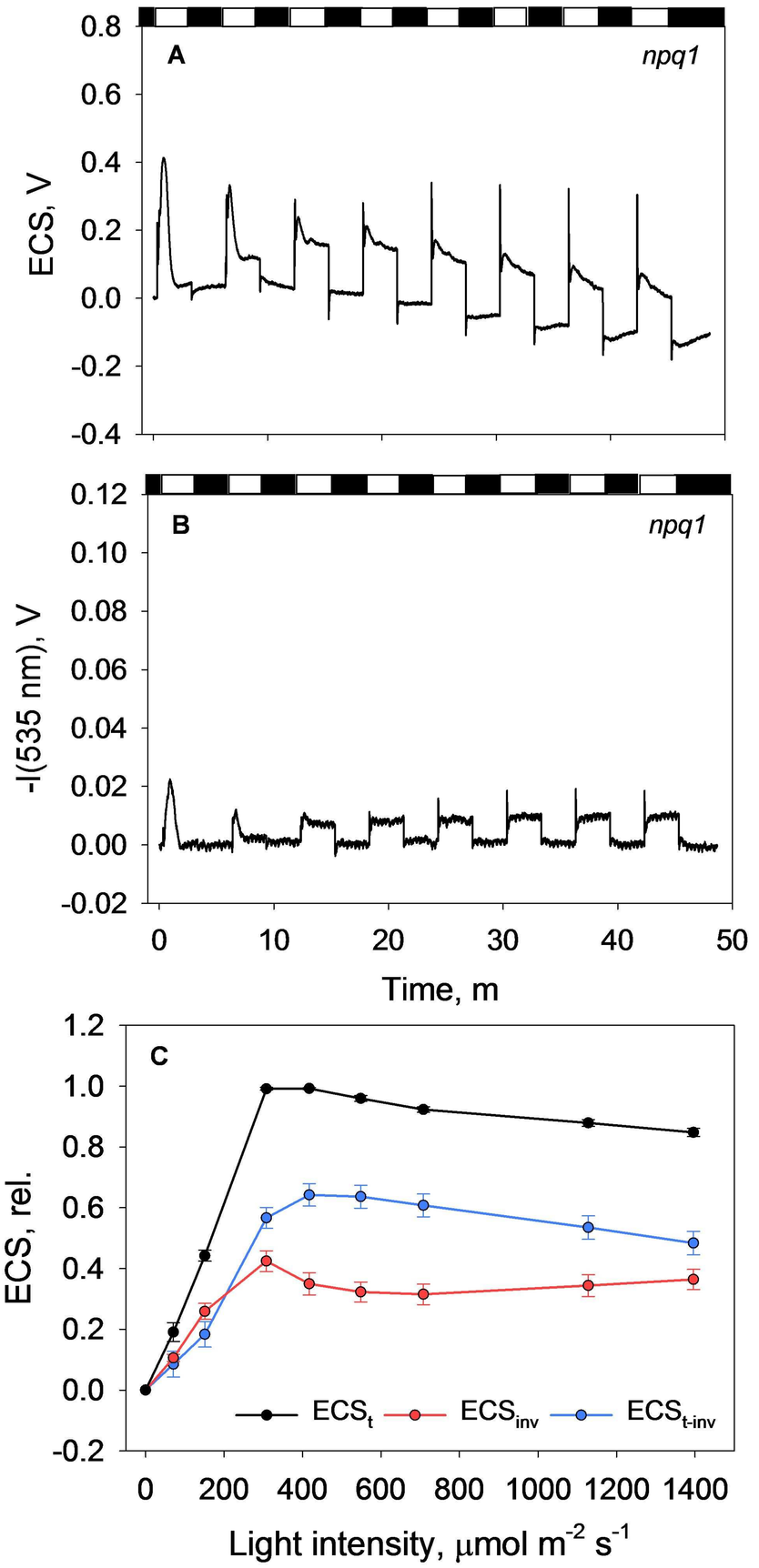

Fig. 3 Electrochromic shift and 535 nm measurements on *npq1* leaves. (A) Representative ECS (ΔA 550 – 515 nm) and (B) ΔA 535 nm kinetics. Each assay consisted of 8 steps of 3 min illumination (white bars) and 3 min darkness (black bars). The illumination increased at each step using 0, 71, 151, 308, 417, 548, 708, 1128, and 1396 μmol photons m^{-2} s^{-1}. (C) ECS$_t$, ECS$_{inv}$, and ECS$_{t-inv}$ at each light intensity. Here, measurements are normalised to the maximum ECS$_t$. Error bars represent SEM (n = 8). ECS, electrochromic shift.

Wilson et al.
Fig. 4

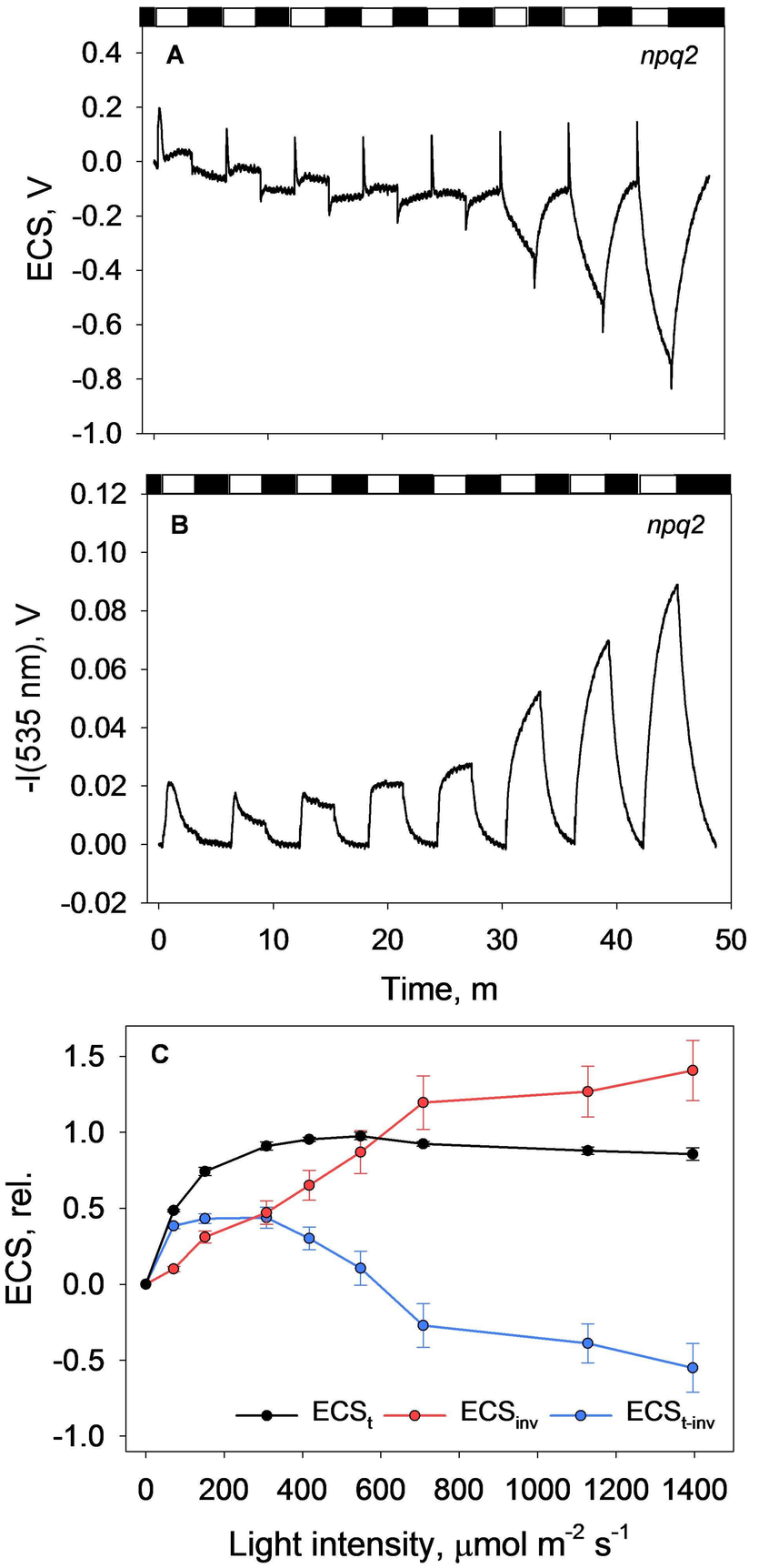

Fig. 4 Electrochromic shift and 535 nm measurements on *npq2* leaves. (A) Representative ECS (ΔA 550 – 515 nm) and (B) ΔA 535 nm kinetics. Each assay consisted of 8 steps of 3 min illumination (white bars) and 3 min darkness (black bars). The illumination increased at each step using 0, 71, 151, 308, 417, 548, 708, 1128, and 1396 µmol photons m^{-2} s^{-1}. (C) ECS_t, ECS_{inv}, and ECS_{t-inv} at each light intensity. Here, measurements are normalised to the maximum ECS_t. Error bars represent SEM (n = 6). ECS, electrochromic shift.

Wilson et al.
Fig. 5

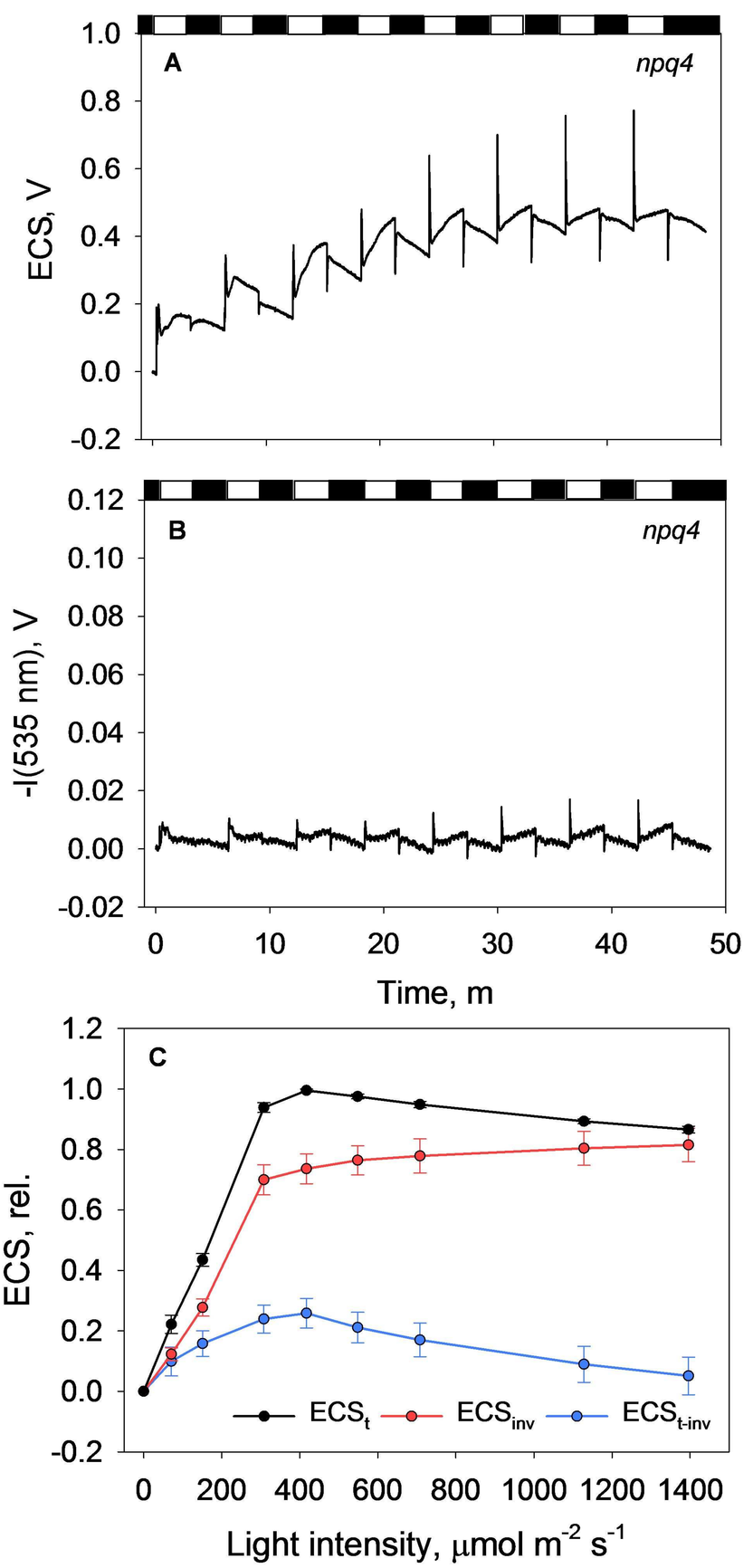

Fig. 5 Electrochromic shift and 535 nm measurements on *npq4* leaves. (A) Representative ECS (ΔA 550 – 515 nm) and (B) ΔA 535 nm kinetics. Each assay consisted of 8 steps of 3 min illumination (white bars) and 3 min darkness (black bars). The illumination increased at each step using 0, 71, 151, 308, 417, 548, 708, 1128, and 1396 µmol photons m^{-2} s^{-1}. (C) ECS_t, ECS_{inv}, and $ECS_{t\text{-}inv}$ at each light intensity. Here, measurements are normalised to the maximum ECS_t. Error bars represent SEM (n = 8). ECS, electrochromic shift.

Wilson et al.
Fig. 6

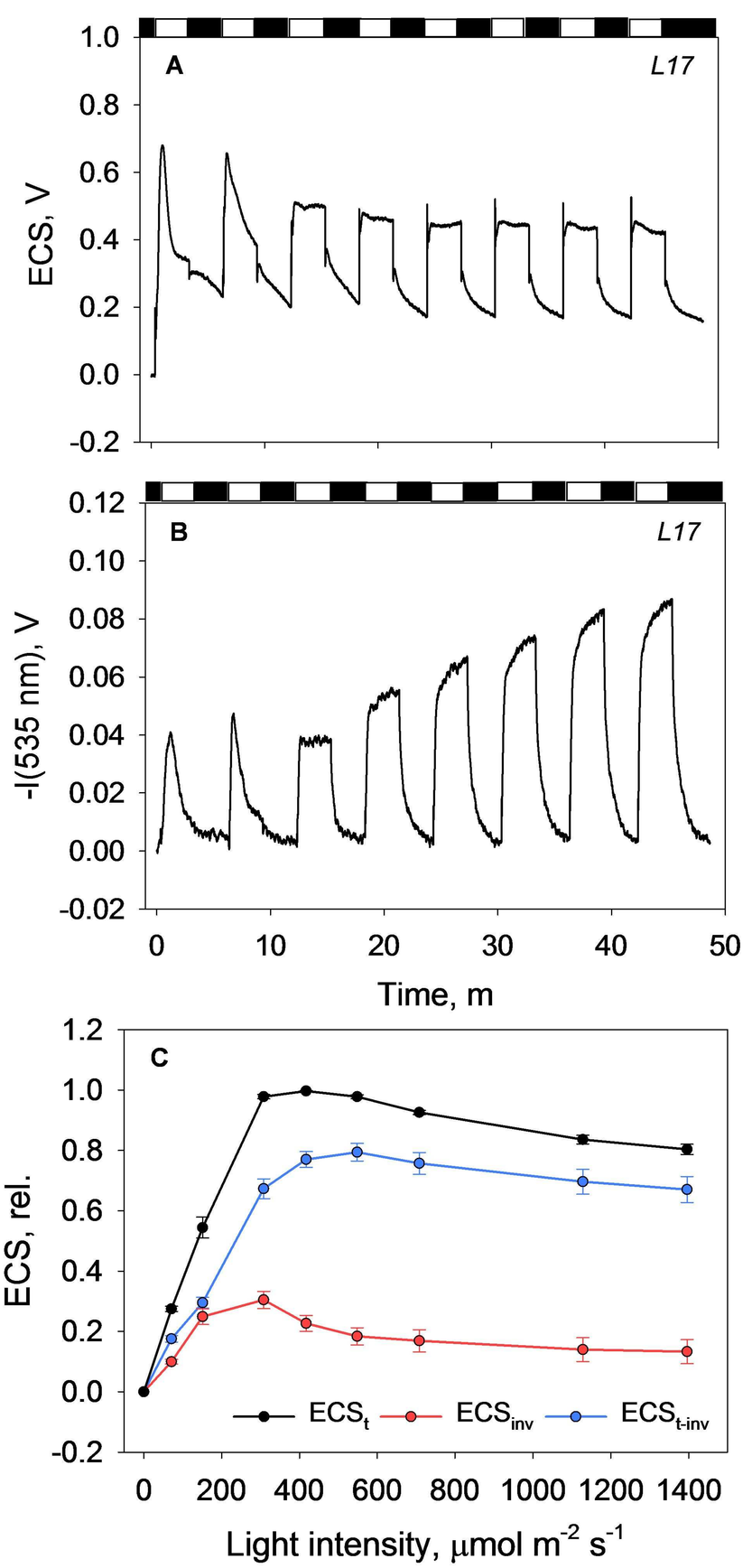

Fig. 6 Electrochromic shift and 535 nm measurements on *L17* leaves. (A) Representative ECS (ΔA 550 – 515 nm) and (B) ΔA 535 nm kinetics. Each assay consisted of 8 steps of 3 min illumination (white bars) and 3 min darkness (black bars). The illumination increased at each step using 0, 71, 151, 308, 417, 548, 708, 1128, and 1396 μmol photons m^{-2} s^{-1}. (C) ECS$_t$, ECS$_{inv}$, and ECS$_{t\text{-}inv}$ at each light intensity. at each light intensity. Here, measurements are normalised to the maximum ECS$_t$. Error bars represent SEM (*n* = 8). ECS, electrochromic

Wilson et al.
Fig. 7

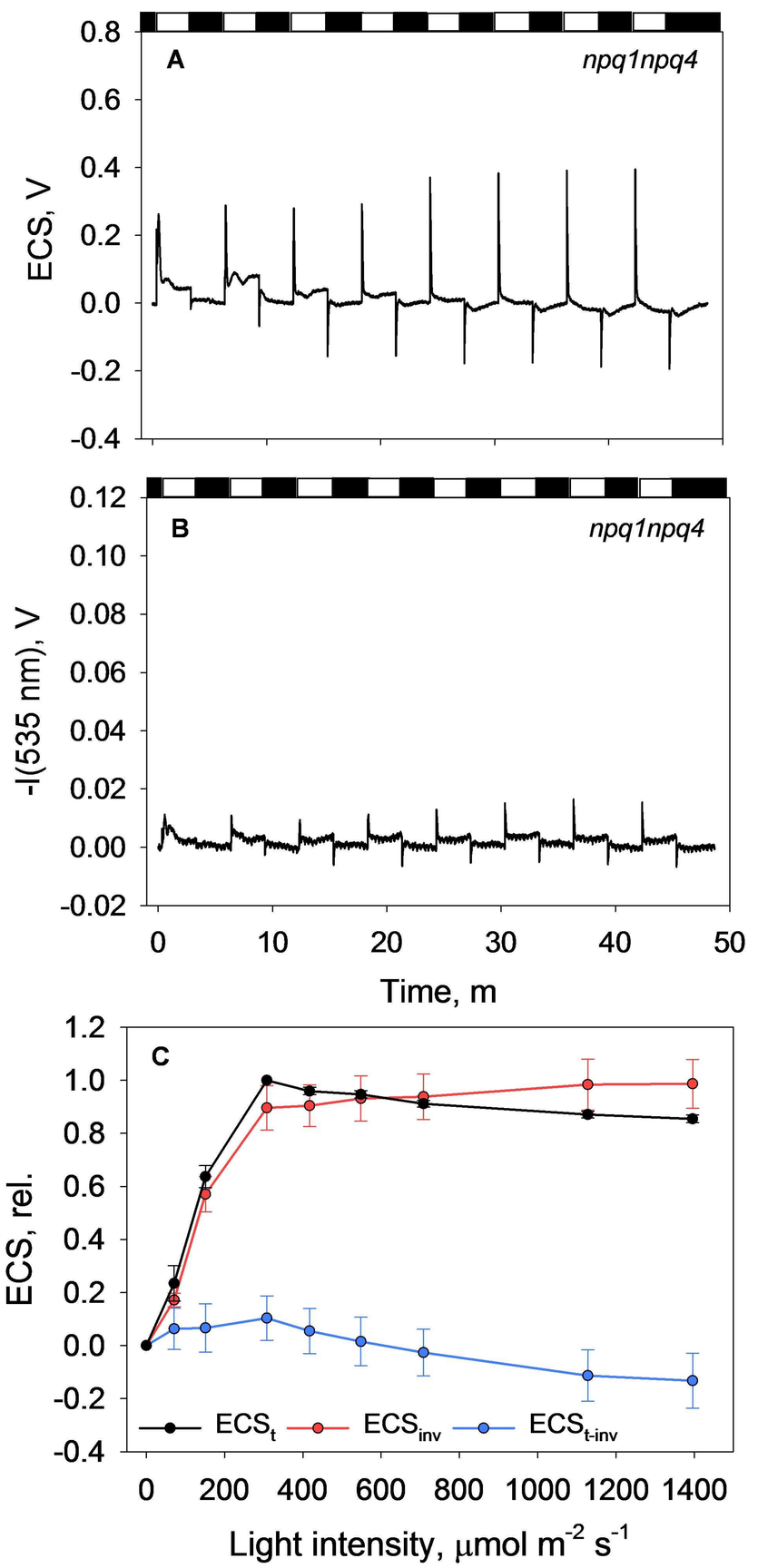

Fig. 7 Electrochromic shift and 535 nm measurements on *npq1npq4* leaves. (A) Representative ECS (ΔA 550 – 515 nm) and (B) ΔA535 kinetics. Each assay consisted of 8 steps of 3 min illumination (white bars) and 3 min darkness (black bars). The illumination increased at each step using 0, 71, 151, 308, 417, 548, 708, 1128, and 1396 µmol photons m^{-2} s^{-1}. (C) ECS_t, ECS_{inv}, and ECS_{t-inv} at each light intensity. Here, measurements are normalised to the maximum ECS_t. Error bars represent SEM (*n* = 5). ECS, electrochromic shift.

Parsed Citations

Armbruster U, Carrillo LR, Venema K, Pavlovic L, Schmidtmann E, Kornfeld A, Jahns P, Berry JA, Kramer DM, Jonikas MC (2014) Ion antiport accelerates photosynthetic acclimation in fluctuating light environments. Nat Commun 5: 1–8
Google Scholar: Author Only Title Only Author and Title

Armbruster U, Correa Galvis V, Kunz HH, Strand DD (2017) The regulation of the chloroplast proton motive force plays a key role for photosynthesis in fluctuating light. Curr Opin Plant Biol 37: 56–62
Google Scholar: Author Only Title Only Author and Title

Armbruster U, Leonelli L, Galvis VC, Strand D, Quinn EH, Jonikas MC, Niyogi KK (2016) Regulation and levels of the thylakoid K+/H+ antiporter KEA3 shape the dynamic response of photosynthesis in fluctuating light. Plant Cell Physiol. doi: 10.1093/pcp/pcw085
Google Scholar: Author Only Title Only Author and Title

Bailleul B, Cardol P, Breyton C, Finazzi G (2010) Electrochromism: A useful probe to study algal photosynthesis. Photosynth Res 106: 179–189
Google Scholar: Author Only Title Only Author and Title

Barber J, Mills J, Nicolson J (1974) Studies with cation specific ionophores show that within the intact chloroplast Mg++ acts as the main exchange cation for H + pumping. FEBS Lett 49: 106–110
Google Scholar: Author Only Title Only Author and Title

Bennoun P (1994) Chlororespiration revisited: Mitochondrial-plastid interactions in Chlamydomonas. BBA - Bioenerg 1186: 59–66
Google Scholar: Author Only Title Only Author and Title

Bilger W, Björkman O (1990) Role of the xanthophyll cycle in photoprotection elucidated by measurements of light-induced absorbance changes, fluorescence and photosynthesis in leaves of Hedera canariensis. Photosynth Res 25: 173–185
Google Scholar: Author Only Title Only Author and Title

Bilger W, Bjorkman O, Thayer SS (1989) Light-Induced Spectral Absorbance Changes in Relation to Photosynthesis and the Epoxidation State of Xanthophyll Cycle Components in Cotton Leaves. Plant Physiol 91: 542–551
Google Scholar: Author Only Title Only Author and Title

Bulychev AA (1984) Different kinetics of membrane potential formation in dark-adapted and preilluminated chloroplasts. Biochim Biophys Acta - Bioenerg 766: 647–652
Google Scholar: Author Only Title Only Author and Title

Bulychev AA, Andrianov VK, Kurella GA, Litvin FF (1972) Micro-electrode Measurements of the transmembrane potential of chloroplasts and its photoinduced changes. Nature 236: 175–177
Google Scholar: Author Only Title Only Author and Title

Carraretto L, Formentin E, Teardo E, Checchetto V, Tomizioli M, Morosinotto T, Giacometti GM, Finazzi G, Szabó I (2013) A Thylakoid-Located Two-Pore K + Channel Controls Photosynthetic Light Utilization in Plants. Science (80-) 342: 114–118
Google Scholar: Author Only Title Only Author and Title

Chow W, Wagner A, Hope A (1976) Light-dependent Redistribution of Ions in Isolated Spinach Chloroplasts. Funct Plant Biol 3: 853
Google Scholar: Author Only Title Only Author and Title

Crouchman S, Ruban A, Horton P (2006) PsbS enhances nonphotochemical fluorescence quenching in the absence of zeaxanthin. FEBS Lett 580: 2053–2058
Google Scholar: Author Only Title Only Author and Title

Cruz JA, Sacksteder CA, Kanazawa A, Kramer DM (2001) Contribution of Electric Field (Δψ) to Steady-State Transthylakoid Proton Motive Force (pmf) in Vitro and in Vivo. Control of pmf Parsing into Δψ and ΔpH by Ionic Strength. Biochemistry 40: 1226–1237
Google Scholar: Author Only Title Only Author and Title

Daum B, Nicastro D, Austin J, McIntosh JR, Kühlbrandt W (2010) Arrangement of Photosystem II and ATP Synthase in Chloroplast Membranes of Spinach and Pea. Plant Cell 22: 1299–1312
Google Scholar: Author Only Title Only Author and Title

Davis GA, Kanazawa A, Schöttler MA, Kohzuma K, Froehlich JE, William Rutherford A, Satoh-Cruz M, Minhas D, Tietz S, Dhingra A, et al (2016) Limitations to photosynthesis by proton motive force-induced photosystem II photodamage. Elife 5: 23–27
Google Scholar: Author Only Title Only Author and Title

Davis GA, Rutherford AW, Kramer DM (2017) Hacking the thylakoid proton motive force for improved photosynthesis: Modulating ion flux rates that control proton motive force partitioning into ΔΨ and ΔpH. Philos Trans R Soc B Biol Sci 372: 20160381
Google Scholar: Author Only Title Only Author and Title

Dilley RA, Vernon LP (1965) Ion and water transport processes related to the light-dependent shrinkage of spinach chloroplasts. Arch Biochem Biophys 111: 365–375
Google Scholar: Author Only Title Only Author and Title

Duan Z, Kong F, Zhang L, Li W, Zhang J, Peng L (2016) Abestrophin-like protein modulates the proton motive force across the

thylakoid membrane in Arabidopsis. J Integr Plant Biol 58: 848–858
Google Scholar: Author Only Title Only Author and Title

Duffy CDP, Johnson MP, Macernis M, Valkunas L, Barford W, Ruban AV. (2010) A theoretical investigation of the photophysical consequences of major plant light-harvesting complex aggregation within the photosynthetic membrane. J Phys Chem B 114: 15244–15253
Google Scholar: Author Only Title Only Author and Title

Duniec JT, Thorne SW (1977) The relation of light-induced slow absorbancy and scattering changes about 520 nm and structure of chloroplast thylakoids-A theoretical investigation. J Bioenerg Biomembr 9: 223–235
Google Scholar: Author Only Title Only Author and Title

Ettinger WF, Clear AM, Fanning KJ, Peck M Lou (1999) Identification of a Ca2+/H+ Antiport in the Plant Chloroplast Thylakoid Membrane. Plant Physiol 119: 1379–1386
Google Scholar: Author Only Title Only Author and Title

Evron Y, McCarty RE (2000) Simultaneous Measurement of ΔpH and Electron Transport in Chloroplast Thylakoids by 9-Aminoacridine Fluorescence. Plant Physiol 124: 407–414
Google Scholar: Author Only Title Only Author and Title

Hahn A, Vonck J, Mills DJ, Meier T, Kühlbrandt W (2018) Structure, mechanism, and regulation of the chloroplast ATP synthase. Science (80-) 360: eaat4318
Google Scholar: Author Only Title Only Author and Title

Hald S, Nandha B, Gallois P, Johnson GN (2008) Feedback regulation of photosynthetic electron transport by NADP(H) redox poise. Biochim Biophys Acta - Bioenerg 1777: 433–440
Google Scholar: Author Only Title Only Author and Title

Hangarter RP, Good NE (1982) Energy thresholds for ATP synthesis in chloroplasts. Biochim Biophys Acta - Bioenerg 681: 397–404
Google Scholar: Author Only Title Only Author and Title

Havaux M, Niyogi KK (1999) The violaxanthin cycle protects plants from photooxidative damage by more than one mechanism. Proc Natl Acad Sci 96: 8762–8767
Google Scholar: Author Only Title Only Author and Title

Herdean A, Nziengui H, Zsiros O, Solymosi K, Garab G, Lundin B, Spetea C (2016a) The Arabidopsis thylakoid chloride channel AtCLCe functions in chloride homeostasis and regulation of photosynthetic electron transport. Front Plant Sci 7: 1–15
Google Scholar: Author Only Title Only Author and Title

Herdean A, Teardo E, Nilsson AK, Pfeil BE, Johansson ON, Ünnep R, Nagy G, Zsiros O, Dana S, Solymosi K, et al (2016b) A voltage-dependent chloride channel fine-tunes photosynthesis in plants. Nat Commun 7: 1–11
Google Scholar: Author Only Title Only Author and Title

Horton P, Ruban AV., Rees D, Pascal AA, Noctor G, Young AJ (1991) Control of the light-harvesting function of chloroplast membranes by aggregation of the LHCII chlorophyll-protein complex. FEBS Lett 292: 1–4
Google Scholar: Author Only Title Only Author and Title

Horton P, Ruban AV., Wentworth M (2000) Allosteric regulation of the light-harvesting system of photosystem II. Philos Trans R Soc B Biol Sci 355: 1361–1370
Google Scholar: Author Only Title Only Author and Title

Ilioaia C, Johnson MP, Duffy CDP, Pascal AA, Van Grondelle R, Robert B, Ruban AV. (2011) Origin of absorption changes associated with photoprotective energy dissipation in the absence of zeaxanthin. J Biol Chem 286: 91–98
Google Scholar: Author Only Title Only Author and Title

Johnson GN (2003) Thiol regulation of the thylakoid electron transport chain - A missing link in the regulation of photosynthesis? Biochemistry 42: 3040–3044

Johnson MP, Perez-Bueno ML, Zia A, Horton P, Ruban AV. (2009) The Zeaxanthin-Independent and Zeaxanthin-Dependent qE Components of Nonphotochemical Quenching Involve Common Conformational Changes within the Photosystem II Antenna in Arabidopsis. Plant Physiol 149: 1061–1075
Google Scholar: Author Only Title Only Author and Title

Johnson MP, Ruban AV. (2014) Rethinking the existence of a steady-state Δψ component of the proton motive force across plant thylakoid membranes. Photosynth Res 119: 233–242
Google Scholar: Author Only Title Only Author and Title

Johnson MP, Ruban AV. (2009) Arabidopsis plants lacking PsbS protein possess photoprotective energy dissipation. Plant J 61: 283–289
Google Scholar: Author Only Title Only Author and Title

Johnson MP, Ruban AV. (2011) Restoration of rapidly reversible photoprotective energy dissipation in the absence of PsbS protein by enhanced ΔpH. J Biol Chem 286: 19973–19981
Google Scholar: Author Only Title Only Author and Title

Johnson MP, Zia A, Ruban AV. (2012) Elevated ΔpH restores rapidly reversible photoprotective energy dissipation in Arabidopsis chloroplasts deficient in lutein and xanthophyll cycle activity. Planta 235: 193–204
Google Scholar: Author Only Title Only Author and Title

Kanazawa A, Kramer DM (2002) In vivo modulation of nonphotochemical exciton quenching (NPQ) by regulation of the chloroplast ATP synthase. Proc Natl Acad Sci 99: 12789–12794
Google Scholar: Author Only Title Only Author and Title

Klughammer C, Siebke K, Schreiber U (2013) Continuous ECS-indicated recording of the proton-motive charge flux in leaves. Photosynth Res 117: 471–487
Google Scholar: Author Only Title Only Author and Title

Van Kooten O, Snel JFH, Vredenberg WJ (1986) Photosynthetic free energy transduction related to the electric potential changes across the thylakoid membrane. Photosynth Res 9: 211–227
Google Scholar: Author Only Title Only Author and Title

Kramer DM, Cruz JA, Kanazawa A (2003) Balancing the central roles of the thylakoid proton gradient. Trends Plant Sci 8: 27–32
Google Scholar: Author Only Title Only Author and Title

Kramer DM, Sacksteder CA (1998) A diffused-optics flash kinetic spectrophotometer (DOFS) for measurements of absorbance changes in intact plants in the steady-state. Photosynth Res 56: 103–112
Google Scholar: Author Only Title Only Author and Title

Kramer DM, Sacksteder CA, Cruz JA (1999) How acidic is the lumen? Photosynth Res 60: 151–163

Krieger A, Weis E (1993) The role of calcium in the pH-dependent control of Photosystem II. Photosynth Res 37: 117–130
Google Scholar: Author Only Title Only Author and Title

Lambert AJ, Brand MD (2004) Superoxide production by NADH:ubiquinone oxidoreductase (complex I) depends on the pH gradient across the mitochondrial inner membrane. Biochem J 382: 511–517
Google Scholar: Author Only Title Only Author and Title

Li X-P, Björkman O, Shih C, Grossman AR, Rosenquist M, Jansson S, Niyogi KK (2000) A pigment-binding protein essential for regulation of photosynthetic light harvesting. Nature 403: 391–395
Google Scholar: Author Only Title Only Author and Title

Li X-P, Müller-Moulé P, Gilmore AM, Niyogi KK (2002) PsbS-dependent enhancement of feedback de-excitation protects photosystem II from photoinhibition. Proc Natl Acad Sci 99: 15222–15227
Google Scholar: Author Only Title Only Author and Title

Lyu H, Lazár D (2017) Modeling the light-induced electric potential difference (ΔΨ), the pH difference (ΔpH) and the proton motive force across the thylakoid membrane in C3 leaves. J Theor Biol 413: 11–23
Google Scholar: Author Only Title Only Author and Title

Malone LA, Proctor MS, Hitchcock A, Hunter CN, Johnson MP (2021) Cytochrome b6f – Orchestrator of photosynthetic electron transfer. Biochim Biophys Acta - Bioenerg 1862: 148380
Google Scholar: Author Only Title Only Author and Title

Metzger SU, Cramer WA, Whitmarsh J (1997) Critical analysis of the extinction coefficient of chloroplast cytochrome f. Biochim Biophys Acta - Bioenerg 1319: 233–241
Google Scholar: Author Only Title Only Author and Title

Mitchell P (1961) Coupling of phosphorylation to electron and hydrogen transfer by a chemi-osmotic type of mechanism. Nature 191: 144–148
Google Scholar: Author Only Title Only Author and Title

Mitchell P (2011) Chemiosmotic coupling in oxidative and photosynthetic phosphorylation. Biochim Biophys Acta - Bioenerg 1807: 1507–1538
Google Scholar: Author Only Title Only Author and Title

Murakami S, Packer L (1970a) Light-induced Changes in the Conformation and Configuration of the Thylakoid Membrane of Ulva and Porphyra Chloroplasts in Vivo. Plant Physiol 45: 289–299
Google Scholar: Author Only Title Only Author and Title

Murakami S, Packer L (1970b) Protonation and chloroplast membrane structure. J Cell Biol 47: 332–51
Google Scholar: Author Only Title Only Author and Title

Nelson N, Junge W (2015) Structure and Energy Transfer in Photosystems of Oxygenic Photosynthesis. Annu Rev Biochem 84: 659–683
Google Scholar: Author Only Title Only Author and Title

Nishio JN, Whitmarsh J (1993) Dissipation of the proton electrochemical potential in intact chloroplasts: II. The pH gradient monitored by cytochrome f reduction kinetics. Plant Physiol 101: 89–96
Google Scholar: Author Only Title Only Author and Title

Niyogi KK, Grossman AR, Björkman O (1998) Arabidopsis Mutants Define a Central Role for the Xanthophyll Cycle in the Regulation of Photosynthetic Energy Conversion. Plant Cell 10: 1121–1134
Google Scholar: Author Only Title Only Author and Title

Oxborough K, Horton P (1988) A study of the regulation and function of energy-dependent quenching in pea chloroplasts. Biochim Biophys Acta - Bioenerg 934: 135–143
Google Scholar: Author Only Title Only Author and Title

Pérez-Bueno ML, Johnson MP, Zia A, Ruban AV., Horton P (2008) The Lhcb protein and xanthophyll composition of the light harvesting antenna controls the ΔpH-dependency of non-photochemical quenching in Arabidopsis thaliana. FEBS Lett 582: 1477–1482
Google Scholar: Author Only Title Only Author and Title

Petersen J, Forster K, Turina P, Graber P (2012) Comparison of the H+/ATP ratios of the H+-ATP synthases from yeast and from chloroplast. Proc Natl Acad Sci 109: 11150–11155
Google Scholar: Author Only Title Only Author and Title

Pick U, Rottenberg H, Avron M (1974) The dependence of photophosphorylation in chloroplasts on ΔpH and external pH. FEBS Lett 48: 32–36
Google Scholar: Author Only Title Only Author and Title

Remiš D, Bulychev AA, Kurella GA (1986) The electrical and chemical components of the protonmotive force in chloroplasts as measured with capillary and pH-sensitive microelectrodes. Biochim Biophys Acta - Bioenerg 852: 68–73
Google Scholar: Author Only Title Only Author and Title

Roach T, Krieger-Liszkay A (2012) The role of the PsbS protein in the protection of photosystems I and II against high light in Arabidopsis thaliana. Biochim Biophys Acta - Bioenerg 1817: 2158–2165
Google Scholar: Author Only Title Only Author and Title

Rottenberg H, Grunwald T, Avron M (1972) Determination of ΔpH in Chloroplasts. 1. Distribution of [14C]Methylamine. Eur J Biochem 25: 54–63
Google Scholar: Author Only Title Only Author and Title

Ruban AV., Horton P (1999) The Xanthophyll Cycle Modulates the Kinetics of Nonphotochemical Energy Dissipation in Isolated Light-Harvesting Complexes, Intact Chloroplasts, and Leaves of Spinach. Plant Physiol 119: 531–542
Google Scholar: Author Only Title Only Author and Title

Ruban AV., Johnson MP, Duffy CDP (2012) The photoprotective molecular switch in the photosystem II antenna. Biochim Biophys Acta - Bioenerg 1817: 167–181
Google Scholar: Author Only Title Only Author and Title

Ruban AV., Pascal AA, Robert B, Horton P (2002) Activation of zeaxanthin is an obligatory event in the regulation of photosynthetic light harvesting. J Biol Chem 277: 7785–7789
Google Scholar: Author Only Title Only Author and Title

Ruban AV, Wilson S (2020) The Mechanism of Non-Photochemical Quenching in Plants: Localization and Driving Forces. Plant Cell Physiol 44: 1–10
Google Scholar: Author Only Title Only Author and Title

Sacharz J, Giovagnetti V, Ungerer P, Mastroianni G, Ruban AV. (2017) The xanthophyll cycle affects reversible interactions between PsbS and light-harvesting complex II to control non-photochemical quenching. Nat Plants 3: 1–9
Google Scholar: Author Only Title Only Author and Title

Sacksteder CA, Kramer DM (2000) Dark-interval relaxation kinetics (DIRK) of absorbance changes as a quantitative probe of steady-state electron transfer. Photosynth Res 66: 145–158
Google Scholar: Author Only Title Only Author and Title

Schreiber U, Klughammer C (2008) New accessory for the DUAL-PAM-100: The P515/535 module and examples of its application. PAM Appl Notes 10: 1–10
Google Scholar: Author Only Title Only Author and Title

Schuldiner S, Rottenberg H, Avron M (1972) Determination of ΔpH in Chloroplasts. 2. Fluorescent Amines as a Probe for the Determination of ΔpH in Chloroplasts. Eur J Biochem 25: 64–70
Google Scholar: Author Only Title Only Author and Title

Slovacek RE, Hind G (1981) Correlation between photosynthesis and the transthylakoid proton gradient. Biochim Biophys Acta - Bioenerg 635: 393–404
Google Scholar: Author Only Title Only Author and Title

Spetea C, Hideg É, Vass I (1997) Low pH accelerates light-induced damage of photosystem II by enhancing the probability of the donor-side mechanism of photoinhibition. Biochim Biophys Acta - Bioenerg 1318: 275–283
Google Scholar: Author Only Title Only Author and Title

Steigmiller S, Turina P, Graber P (2008) The thermodynamic H+/ATP ratios of the H+-ATPsynthases from chloroplasts and Escherichia

coli. Proc Natl Acad Sci 105: 3745–3750
Google Scholar: Author Only Title Only Author and Title

Suorsa M, Grieco M, Järvi S, Gollan PJ, Kangasjärvi S, Tikkanen M, Aro EM (2013) PGR5 ensures photosynthetic control to safeguard photosystem I under fluctuating light conditions. Plant Signal Behav 8: 167–172
Google Scholar: Author Only Title Only Author and Title

Takizawa K, Cruz JA, Kanazawa A, Kramer DM (2007) The thylakoid proton motive force in vivo. Quantitative, non-invasive probes, energetics, and regulatory consequences of light-induced pmf. Biochim Biophys Acta - Bioenerg 1767: 1233–1244
Google Scholar: Author Only Title Only Author and Title

Tikkanen M, Rantala S, Aro EM (2015) Electron flow from PSII to PSI under high light is controlled by PGR5 but not by PSBS. Front Plant Sci 6: 1–6
Google Scholar: Author Only Title Only Author and Title

Townsend AJ, Saccon F, Giovagnetti V, Wilson S, Ungerer P, Ruban AV. (2018) The causes of altered chlorophyll fluorescence quenching induction in the Arabidopsis mutant lacking all minor antenna complexes. Biochim Biophys Acta - Bioenerg 1859: 666–675
Google Scholar: Author Only Title Only Author and Title

Vredenberg WJ (1997) Electrogenesis in the photosynthetic membrane: Fields, facts and features. Bioelectrochemistry Bioenerg 44: 1–11
Google Scholar: Author Only Title Only Author and Title

Vredenberg WJ, Bulychev AA (1976) Changes in the electrical potential across the thylakoid membranes of illuminated intact chloroplasts in the presence of membrane-modifying agents. Plant Sci Lett 7: 101–107
Google Scholar: Author Only Title Only Author and Title

Wilson S, Ruban AV. (2020) Enhanced NPQ affects long-term acclimation in the spring ephemeral Berteroa incana. Biochim Biophys Acta - Bioenerg 1861: 148014
Google Scholar: Author Only Title Only Author and Title

Wilson S, Ruban AV. (2019) Quantitative assessment of the high-light tolerance in plants with an impaired photosystem II donor side. Biochem J 476: 1377–1386
Google Scholar: Author Only Title Only Author and Title

Witt HT (1971) Coupling of quanta, electrons, field ions and phosphorylation in the functional membrane of photosynthesis. Quart Res Biophys 4: 365–477
Google Scholar: Author Only Title Only Author and Title

Witt HT (1979) Energy conversion in the functional membrane of photosynthesis. Analysis by light pulse and electric pulse methods. Biochim Biophys Acta - Rev Bioenerg 505: 355–427
Google Scholar: Author Only Title Only Author and Title

Wolf DM, Segawa M, Kondadi AK, Anand R, Bailey ST, Reichert AS, Bliek AM, Shackelford DB, Liesa M, Shirihai OS (2019) Individual cristae within the same mitochondrion display different membrane potentials and are functionally independent. EMBO J 38: 1–21
Google Scholar: Author Only Title Only Author and Title

Yamamoto H, Shikanai T (2020) Does the Arabidopsis proton gradient regulation5 Mutant Leak Protons from the Thylakoid Membrane? Plant Physiol 184: 421–427

Yamamoto HY, Wang Y, Kamite L (1971) A chloroplast absorbance change from violaxanthin de-epoxidation. A possible component of 515 nm changes. Biochem Biophys Res Commun 42: 37–42
Google Scholar: Author Only Title Only Author and Title

Zaharieva I, Wichmann JM, Dau H (2011) Thermodynamic limitations of photosynthetic water oxidation at high proton concentrations. J Biol Chem 286: 18222–18228
Google Scholar: Author Only Title Only Author and Title